THE UNIVERSITY OF MICHIGAN

COLLEGE OF ENGINEERING
Department of Engineering Mechanics
Department of Mechanical Engineering

Tire and Suspension Systems Research Group

Translation No. 1

INVESTIGATIONS OF AUTOMOBILE TIRES

Dr.-Ing. G. Krempl

Translated by Eugen Füner and S.K. Clark

ORA Project 08904

administered through:

OFFICE OF RESEARCH ADMINISTRATION ANN ARBOR

July 1968

The original articles appeared in the magazine

Automobiltechnische Zeitschrift, Vol. 69, No. 1,

January 1967, and Vol. 69, No. 8, August 1967.

A general description has appeared in previous publications (21, 34) of a new test apparatus constructed at the institute of Professor K. Kollmann, Technische Hochschule Karlsruhe. Here, the tire is mounted inside a drum of about 4 meters diameter. In a later paper (1965), the construction of this entire device was fully described together with some preliminary results from it.

PART I

THE TEST STAND

Many different test methods are used to determine the characteristics of automobile tires. Running the tire on the vehicle itself may be considered the oldest method of investigation (3, 10, 28, 55). It is extremely difficult to maintain constant test conditions with this method, since frequent weather changes can occur, and uneveness or waviness of the road surface influences the load on the wheel so that this load is not a constant. As a consequence, load oscillations occur at some high frequency. In addition to this, the mean or average load on the wheel is limited by the weight of the vehicle, if one uses the vehicle as a testing device. Twist and elastic deformation of the chassis as well as the action of the suspension, and the steering system both greatly influence measurements made on the highway. Nevertheless, this technique will always be valuable and necessary for assessing the performance of a vehicle. The development of tire measuring trailers for roadway experiments has helped remove many of these difficulties (12, 15, 16, 38, 41, 47, 49, 50, 52). These measuring trailers have worked well, and are particularly valuable for determining the friction coefficients between tire and roadway.

Most of the measurements of tangential forces on tires are performed on test drums or test wheels (4, 27, 28, 30, 44, 50). Generally these test drums use the external surface and have diameters up to 2.5 meters. In such test devices, it is easy to change parameters such as inflation, pressure, load, camber, and steer angle so that a map of tire characteristics may be easily and quickly determined. Since one may apply indefinitely large forces, such characteristics can be investigated up to the limits of tire rupture.

Due to the curvature of the test drum, and its steel surface, test results deviate from those obtained on a flat roadway. In the literature there is apparently no clear-cut statement of how drum data deviates from roadway data. Comparative measurements now available in various publications indicate contradictory trends. For example, Gaus (16) obtained side forces on a steel drum which are ten to fifteen percent greater than on a roadway, while the measurements of Gough on the steel drum lie about 10% below those obtained on the road, and those of Joy and Hartley (26) are about 17% below those obtained on the road. Bull (4) gets similar results and his measurements must take preference since they are based on identical surface textures of the drum and pavement. He used emery paper for all surfaces and thus eliminated the influence of different friction coefficients. His measurements gave smaller transverse forces on the curved drum

than on flat plane up to a steer angle of 4°. Comparative measurement taken on the inside of drums are not yet available.

Measurements of rolling and slipping losses (3, 6, 11, 30, 40, 42, 43) as well as of side force characteristics in yawed rolling (4, 15, 17, 20, 23, 37, 39, 44, 45, 50, 54, 56) have been known for many years. The designers of tires and vehicles may use these characteristics in making overall comparisons of the influence of different tires. Kamm (24, 28) has investigated the problem of the tire under tractive or braking forces. The measurements were taken from small tire models initially at rest. These models were made of solid rubber of various stiffnesses. The results led to the concept of the circle of friction, as shown in Figure 1. These experiments with models were supplemented by measurements taken from rolling automobile tires by Dietz and others (10). It was found that the transverse or side forces could increase with very small braking forces. One must assume that this phenomena comes about due to the way in which this experiment was performed, since considerable scatter was present in the data. Experimenting on the road with a skid trailer, Forster (12) found in two series of measurements using various braking forces, all other conditions being constant, that the resultant force calculated from the vector addition of transverse and braking force actually changed magnitude with direction. These results, of course, contradict the hypothesis derived from the model experiments, namely that maximum coefficient of friction between wheel and pavement is independent of direction.

Bull (4), and later on Gaus (16), confirmed the effects reported by Dietz, that with small braking forces the side force may increase whereas a tractive force results in a decrease of the possible side forces. Even with all of this information it still is not possible to obtain a general law of frictional effects, since each of the observations reported were derived from separate measurements. In direct contradiction to these measurements, which were made some time ago, Tschudakow (50) states that the side force remains almost constant, and independent of the magnitude of the tractive or braking force for all values below a certain magnitude of the circumferential or braking force. Above this level of braking or tractive force, the side force decreases and finally approaches the same value for all yaw angles. This portion of the curve is a segment of a circle which represents the circle of friction, since the maximum side force approximately equals the maximum braking or tractive force. In contradiction to Forster, this reference concludes that the maximum coefficient of friction is independent of whether the tire is being braked or under a tractive force, and that the side forces were not influenced in magnitude by the braking or tractive forces.

The results of Freeman (13) and the work of Bergman (1) concerning the side force on a tire during acceleration contradict Tschudakow's observations for small circumferential forces. For small steer angles, Freeman and Bergman found that the side force decreased at first proportional to the increase of the tractive force. As soon as the tractive force approached the maximum friction force produced by the tire, the side force further decreased and finally

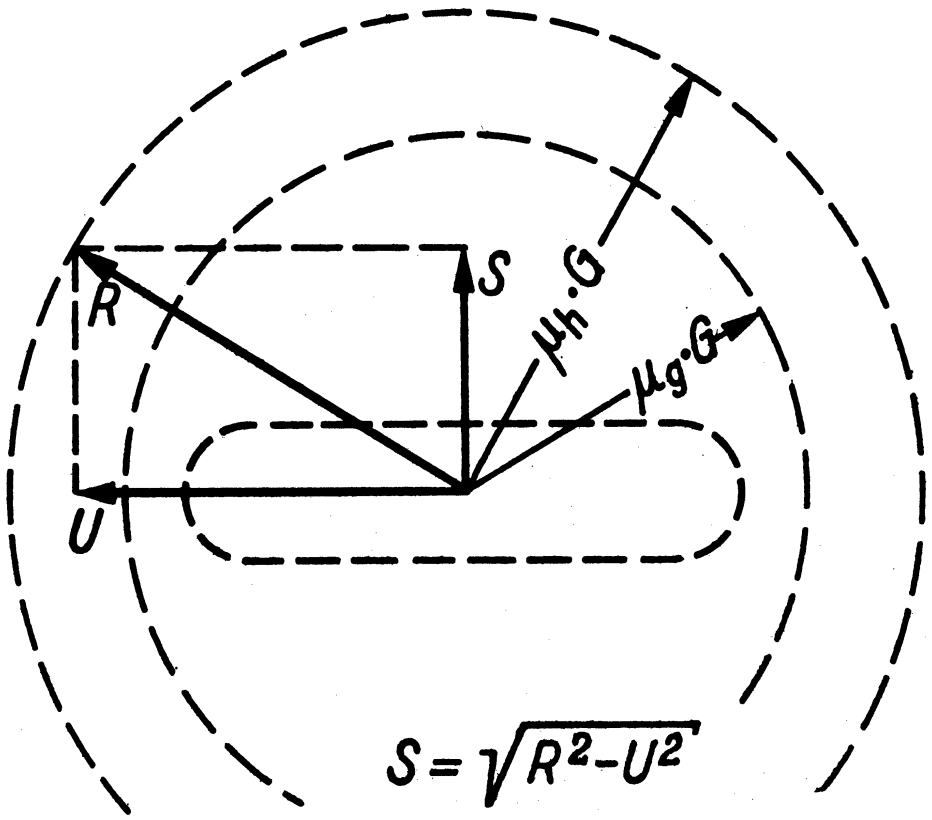

Fig. 1. Definition of the circle of friction. S = side force (transverse force). R = resultant friction force. U = tractive or braking force.

went to zero. Bergman concludes that the gradual decrease of the side force for small tractive forces was caused by the decay of the side force spring rate. Continued decrease of side force, with increasing tractive force is presumed to be due to the reduction of side force friction coefficient.

For purposes of calculating side forces Bergman uses a model of the tire made up of a three-dimensional system of springs. This permits describing tire deformations in three directions, lateral or side deformations, radial deformations and shear deformation in the circumferential direction. In taking into account interactions of the spring systems resulting from these deformations in the three principle directions, these calculations give good agreement with measured data within the range of static friction. The transition from the static friction range to the dynamic friction range was not considered in calculations for circumferential force, so that the side forces asymptotically approached the point of maximum circumferential force. According the Bergman's calculations, this results in the circumferential force influencing the axial force, but on the other hand it allows no feedback on the circumferential force itself. Freeman's data did not include this range of maximum friction coefficient.

CONSTRUCTION OF THE TEST STAND

Purpose

The general requirement which should be fulfilled by any test stand is that it should simulate as closely as possible real driving conditions. The quality of the equipment depends on the possibility of obtaining all necessary measurements easily, and with accuracy and reproducibility.

During a preliminary design study (33, 34) fundamental designs of test stands for tires have been examined critically:

1) drum with external tract

2) drum with internal tract

3) test conveyor or flat belt

4) test disk

5) test stand with flat plank machine.

The design of the device should accommodate the following requirements:

a) the normal velocity — satisfied by design 1, 2, 3, 4

b) flat pavement — satisfied by design 3, (4), 5

c) possibility of changing running surface texture — satisfied by design (1), 2, 4, 5

d) hydroplaning with definite fluid-layer thickness — satisfied by design 2.

With the exception of requirement b), the drum with the internal track fulfills all these requirements. Therefore, an investigation was carried out concerning the influence of the drum curvature on the contact area of the tire. This influence has been kept small by choosing a fairly-large diameter for the wheel, namely 3.8 meters. A track speed of about 25 km/h is sufficient to maintain layers of constant thickness of liquid, since at about 20 km/h the centrifugal acceleration is 1 g. Since hydroplaning appears only at higher velocities, the minimum velocity is 25 km/h does not hamper these studies. This is also true for measurements on gravel, sand, and so on, since due to centrifugal forces tract surfaces can be attached very simply by cementing. It was desired to study not only the rolling tire, but also the influence of braking and tractive forces on tire characteristics. For this purpose, the three force and moment components resulting from the six degrees-of-freedom of the wheel must be measured. The design of the wheel suspension described below was dictated by the requirement to arbitrarily vary steering angle, camber, tire load and air pressure and, of course, the size and fabric of the tires.

INFLUENCE OF DRUM CURVATURE ON THE GEOMETRY OF THE CONTACT AREA

Preliminary experiments and calculations were made concerning the influence of drum curvature, with both inside and outside tracks, on the geometry of the tire contact area. These led to estimates of the ratio of maximum radial deflection on the drum to those on the plane road, and gave an idea of how these differences could be minimized by enlarging the drum diameter. The contact area of geometry was measured as a function of load and air pressure for a series of test tires on both concave, and convex surfaces of different radial curvature. These measurements were compared with calculations done earlier (33, 34), as shown in Figures 2 through 5. Calculations and measurements agree very well, so that the calculations seem to give good estimates of the influence of drum curvature on the deflection of a tire and on the geometry of the contact area.

Figure 6 shows the influence of drum curvature on the deflection f of the tire, and on the length of the contact area L, these quantities being important in sizing the drum for a test stand. Obviously one cannot choose indefinitely large drum diameters. Above a ratio $\frac{R}{r} = 6$ the benefits are not as great as the increasing costs of construction. For tires studied in this paper, R/r lies between 5.5 and 6.0 (5.60-15 to 6.00-15).

The difference between the maximum deflection f on the drum and on a flat plane is only a matter of millimeters. Since this is so small, it appears to be more important to include the larger influence of the change of contact area

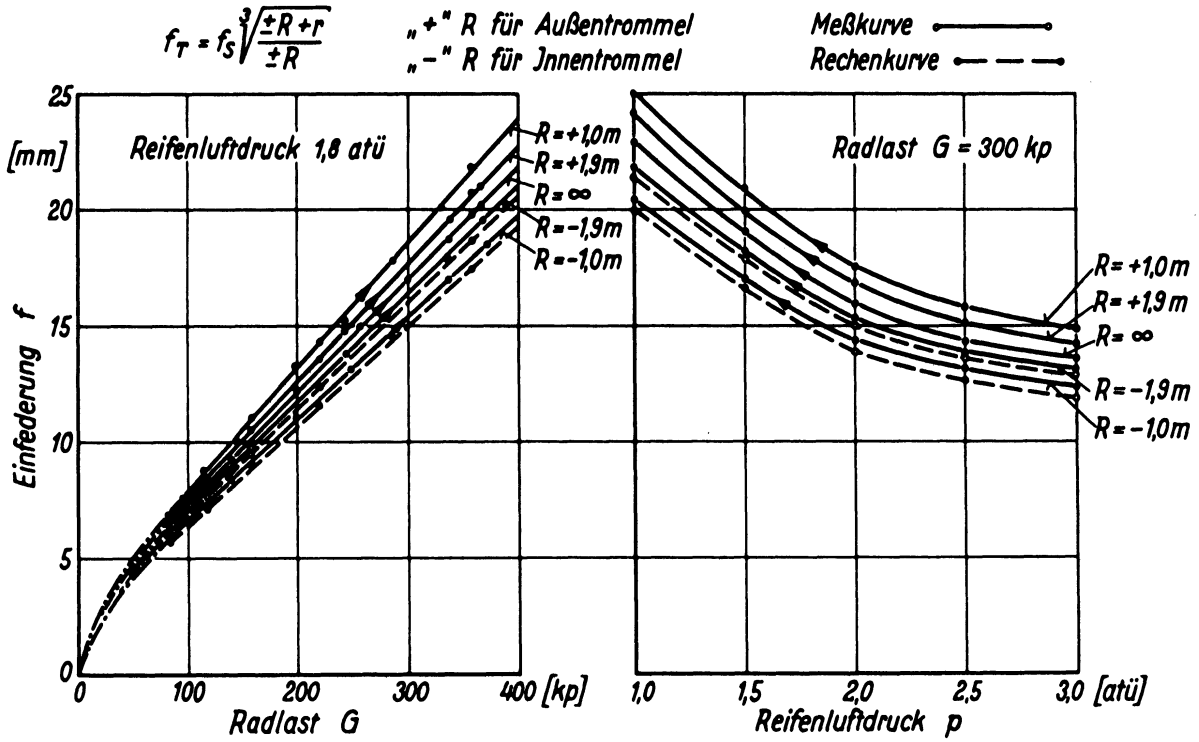

Figs. 2 and 3. Influence on the tire deflection f of the tire load, air pressure and drum curvature for a 6.00-15 tire with 100% profile. f_T = deflection on the drum. f_S = deflection on the road. R = drum radius. r = tire radius.

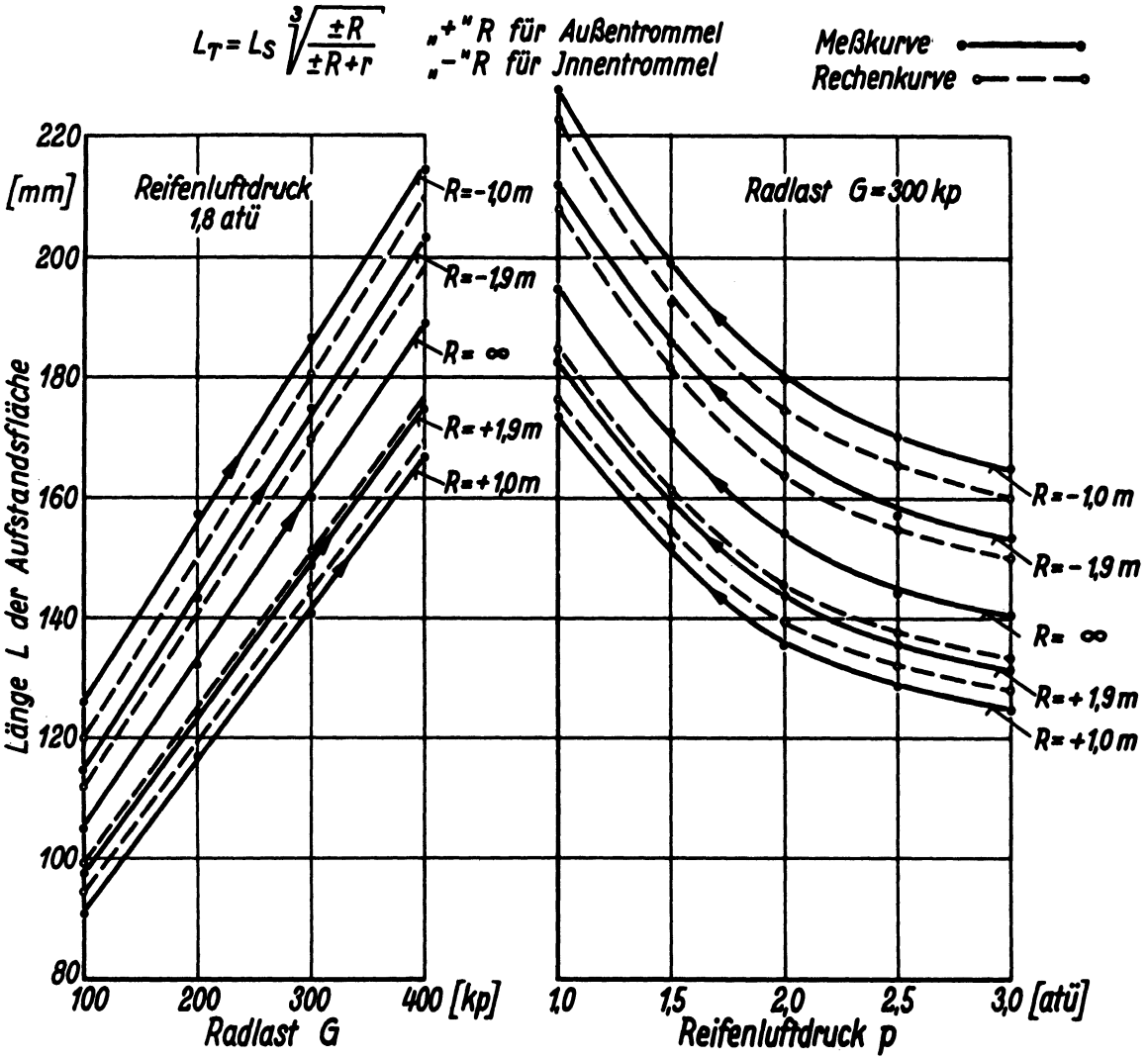

Figs. 4 and 5. Influence on contact patch length L of the tire load, air pressure and drum curvature for a 6.00-15 tire with 100% profile.

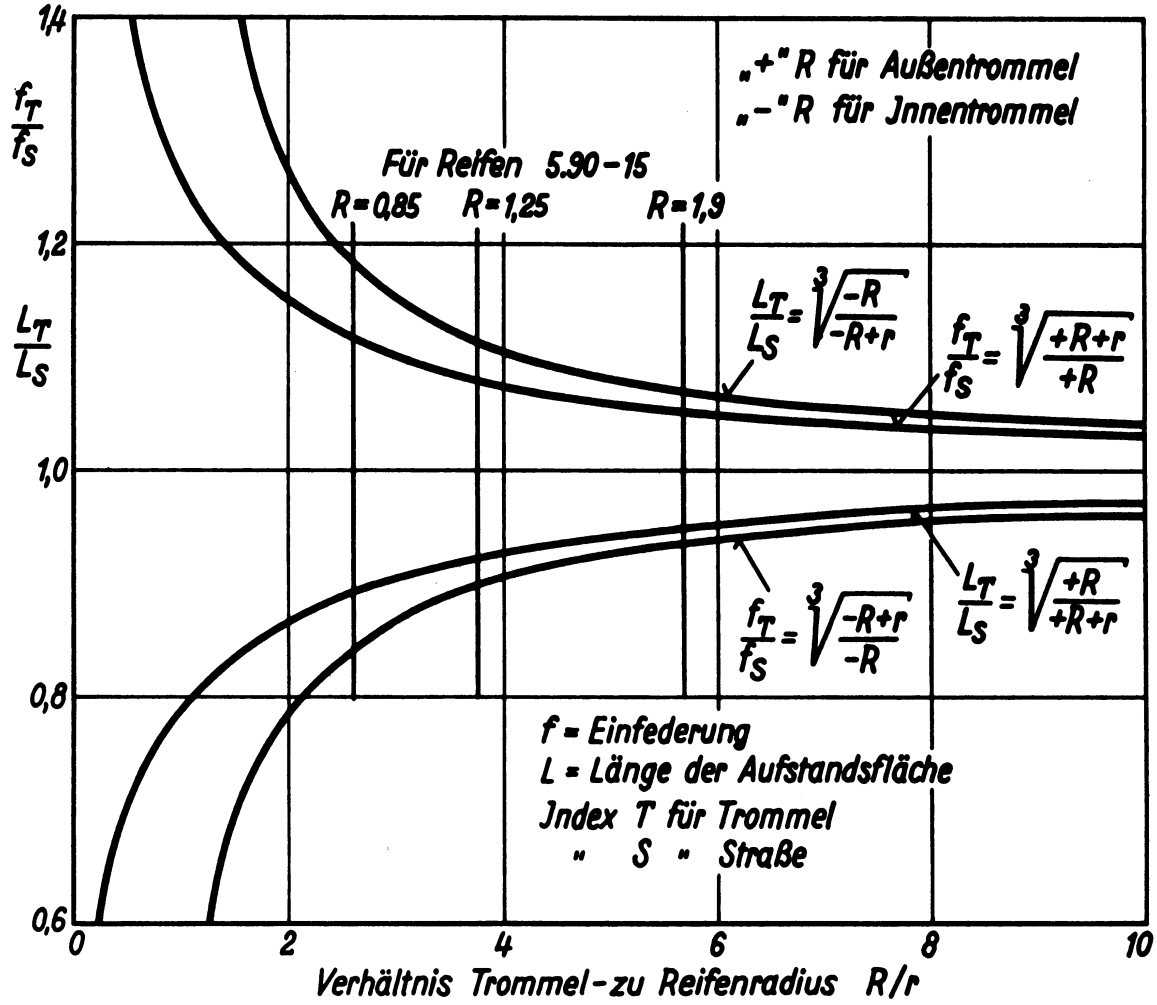

Fig. 6. The influence of the drum curvature on tire deflection f and contact patch length L for different tire radii r and drum radii R.

between the two surfaces in assessing transverse or sideward forces on flat and curved drums respectively. Thus, one of the tires tested (Figures 4 and 5) loaded with 300 kp has on the outside surface of the one meter radius drum a contact patch length of 165 mm at an inflation pressure of 1.15 atmosphere, while on the inside surface of the same drum it has the same contact patch length when inflated with 3.0 atmospheres. Using a constant pressure of 1.8 atmospheres, and a drum radius of 1 meter, a load of 390 kp for the tire on the outside of the drum gave the same length of contact patch as a load of 230 kp for the tire running on the inside of the drum. Corresponding relations for the average pressures in the contact area are given in Figures 7 and 8.

It has been proposed to reduce the air pressure in experiments on the outside of the drum (32). This would create a situation similar in the contact area to that existing when the tire runs on a flat surface. Similarly, one would have to increase the air pressure while running a tire on the inside of the drum. In fact, Figure 8 shows that one may obtain the same average pressure in the contact area on a curved drum surface as on a plane surface. For a 6.00-15 tire with 300 kp load one must reduce the air pressure when running the tire on the outside of a drum of radius R = + 1.0 m (R = + 1.9 meters) about 5% to 9% (3% to 5%) while for the same tire running on the inside of the drum with radius R = -1.0 meters (R = -1.9 meters) one must raise the pressure 6% to 10% (3% to 5%).

Comparative measurements of tires on test drums of different design showed that side forces generated by running the tires on the outside of the drum were always smaller than running tires on a flat pavement of the same surface structure. Since a lower air pressure also reduces side forces, one might, as has been suggested by Menger (32), create in these experiments approximately equal areas of contact, but unfortunately the influence of both factors is to simultaneously reduce the value of the side forces relative to those on a plane track. Therefore, it may be concluded that it is not the average pressure $\bar{p}$ which is important for side forces on a tire, but rather the ratio of p_{max} to $\bar{p}$. It is obvious that $p_{max}/\bar{p}$ is greater on the outside surface of the drum than on a flat track or even on inside of the drum, since p_{max} depends heavily f_{max}.

THE TEST DRUM AND ITS DRIVE MECHANISM

The design of the apparatus is shown in Figure 9. The drum (4) is driven by a DC motor (1) of 110 kw power at 1500 rpm. The motor has continuous speed control by means of a Ward-Leonard device. A six-speed truck transmission allows a number of torque values to be applied to the drum and also allows very low speed to be obtained. A constant step down gear (2) is added, corresponding to the ratio of the drum and test tire diameter. Thus the DC motor and the test tire run at approximately the same speed. For simplicity, a heavy duty truck rear axle was used with the differential blocked off in such a way that this axle can be used as a right angled transmission.

Between the transmission and the drum a torsion measuring hub (3) provides

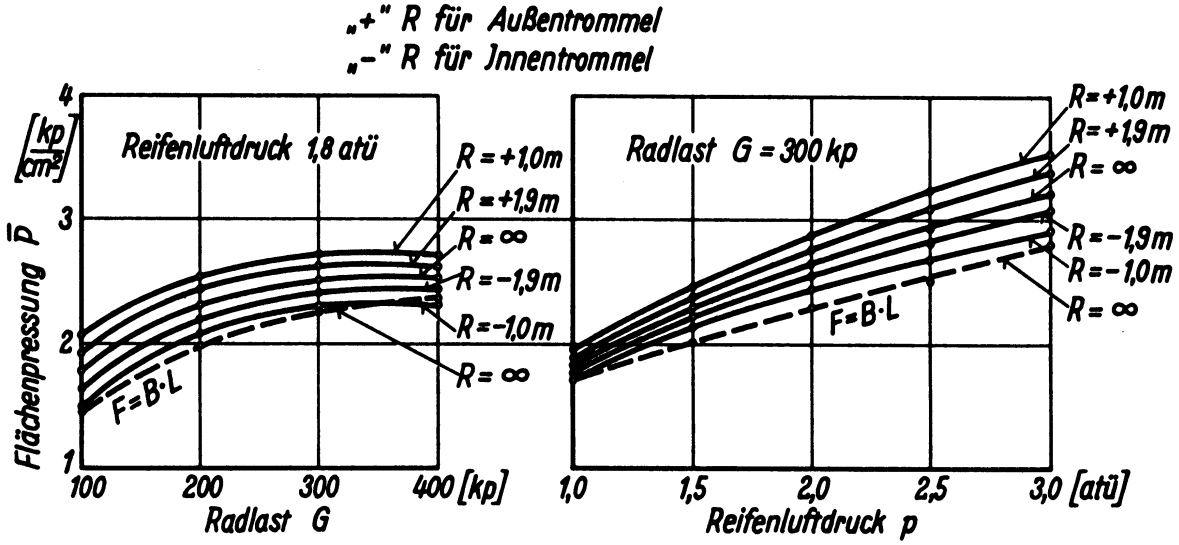

Figs. 7 and 8. Influence of drum curvature on the mean contact pressure $\bar{p} = G/F$, along with variations in the tire load and air pressure for a 6.00-15 tire with 100% profile. B = average width of contact patch. L = length of contact patch.

a measure of torque acting on the shaft. The data is obtained in binary code and is fed out with a set of slip rings (5), from which it is transmitted into a binary decoder which displays the torque reading.

Design radial loads for the test tire are up to 1,000 kg, while the resulting side forces are minor compared to centrifugal forces insofar as drum stresses are concerned.

THE TEST WHEEL AND ITS DRIVING MECHANISM

The test wheel is mounted together with its hub, suspension, loading mechanism, measuring and driving apparatus on a frame (17). The two roller bearings of the frame are preloaded and therefore are free of axial and radial motion. The axis of rotation was carefully centered below the geometric center of contact area and on the axis of the drum. Since both bearings have the same center of pressure, the frame can be supported without stress on two rollers run on a curved rail. The frame can be rotated by a friction transmission (18) which gives two constant velocities. This allows a continuous as well as "step-wise" change of the steer angle. This angle may be read off a scale (14) using a light beam. Because of the optical length available here, the accuracy of the slip angle is plus or minus one minute.

The main frame (16) is situated on the fundamental frame. It can be raised by four eccentric rollers and the test wheel can be drawn back about one meter in order to allow for easy assembly. In a running position this main frame is locked together with the fundamental frame. The test wheel can be raised pneumatically by the unloading mechanism (19) which is attached to the main frame, and can be easily lowered on the running drum without impact. The arm (19) of the unloading mechanism serves as a protective member for the test wheel such that, in the case of a tire defect, the rim will not come in contact with the drum.

The motor for the test wheel (12) has power of 110 kw at 1500 rpm. Together with clutch and the transmission (10) it is mounted on a swinging frame which also is supported by the main frame (15). The driving and braking moments acting on the test wheel are counterbalanced by a measuring member (13). The frame (15) is centered in the main frame (16) and makes up, together with a front and rear tip frame, a hinged parallelogram. These frames remain parallel for any camber adjustment. The camber is adjusted by the spindles which are connected with the front tip frame. The hinges of the two tip frames are level with the track and the drum. Thus there are no relative movements with respect to the drum in the area of contact or in the change of the camber, since the test wheel itself is also suspended by parallel arms.

The angle of camber may be read off the scale at the main frame. The scale reads one degree for every ten millimeters and therefore is usable only for coarse adjustments. For fine adjustments the spindles are provided with very accurate marks for each full degree. The different sizes of tires made the possibility of

vertical movements of the frame (15) necessary. Therefore, two lift spindles are built into the two tip frames. Both lift spindles are driven by worm gears which are connected by a drive shaft. The lift spindles also allow one to level the rear steering joints of the triangular shaped steering arms. One should eventually be able to read the tire sizes from the size of these adjustments. Figures 9 through 11 give a survey of the entire test appartus.

THE WHEEL SUSPENSION

The hub construction and wheel suspension are illustrated in Figures 12 and 13. The braking and driving torques are transmitted to the hub (5) by two Rzeppa joints (6), and the drive shaft. The center of the Rzeppa joint inside the hub lies in the mid-plane of the wheel. The play of the hub is adjusted by two cone-type bearings. The distance between the two joints is exactly equal to the length of the two triangular shaped steering arms (8 and 9). This helps to avoid displacements by changes of the length of the drive shaft during positioning of the test wheel. The rear Rzeppa joint is held by a leaf spring coupling (item 9 of Figure 9), which is very soft in the axial direction but torsionally rigid. Thus no axial forces may be transmitted through the drive shaft. To avoid camber changes during positioning the test wheel, the hub of the test wheel is extended by means of two ball joints and two triangular shaped steering arms, each of 650 millimeters length. This arrangement gives only very small axial displacement in the contact area even with large deflections of the test wheel during positioning. The four joints (10) which suspend the steering arms in the frame are connected with the appartus for measuring side forces, circumferential forces, the camber moment and the friction moment in the hub bearings.

The measuring apparatus, Figure 14, is kept horizontal by the hinge (4) and the rear transverse steering system for all values of camber. The forces are transmitted through the measuring element (5) which deflects as a beam by means of the double tension rod support. The two tension rods transmit the vertical forces and the horizontal circumferential forces directly to the frame, while the axial horizontal forces act on the beam (5). The tension rod support allows a frictionless measurement of circumferential and side forces. During calibration no significant hysteresis was detected. The beam (5) can be replaced by other beams of different sensitivity. The tire is loaded by a coil spring (Part 6, Figure 9) which is attached to the frame by a spindle. The load acts on the lower triangular steering arm and hence through a load cell which is kept vertical by a special guide. Thus, feedback effects on the measurements of circumferential side forces are avoided. Springs of different spring rates are available for different load ranges. If damping is desired the spring may be combined with a shock absorber in parallel. The loading equipment is designed so that the coil springs may be replaced by hydraulic or pneumatic systems, in the event that the load on the wheel approaches a 1,000 kp.

The test wheel may be rotated through another plus or minus 5 degrees over and above the steer angle available from the fundamental frame. This additional

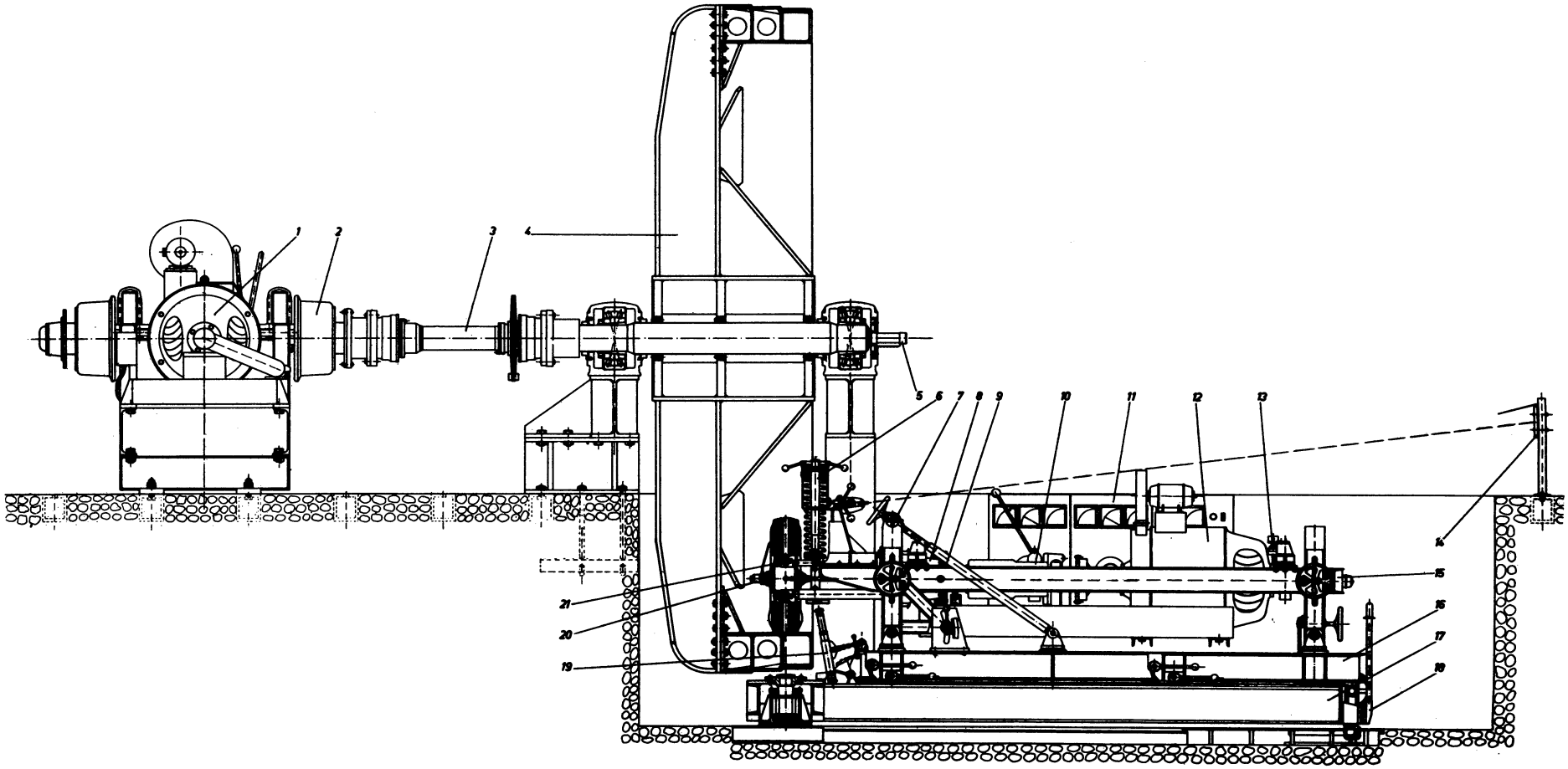

Fig. 9. Test stand for tires at the Technische Hochschule Karlsruhe. The shaft of the drum is anchored in two swinging roller bearings and connected with the hub by means of three compression rings. The third bulkhead in the middle allows one to use a relatively slender shaft (200 mm in dia) whose deflection is only 0.05 mm under a drum load of 7.5 t maximum. The welded drum is bolted onto 8 I-shaped spokes. Other details are given in the text. Scale 1:40, total length about 9.5 m.

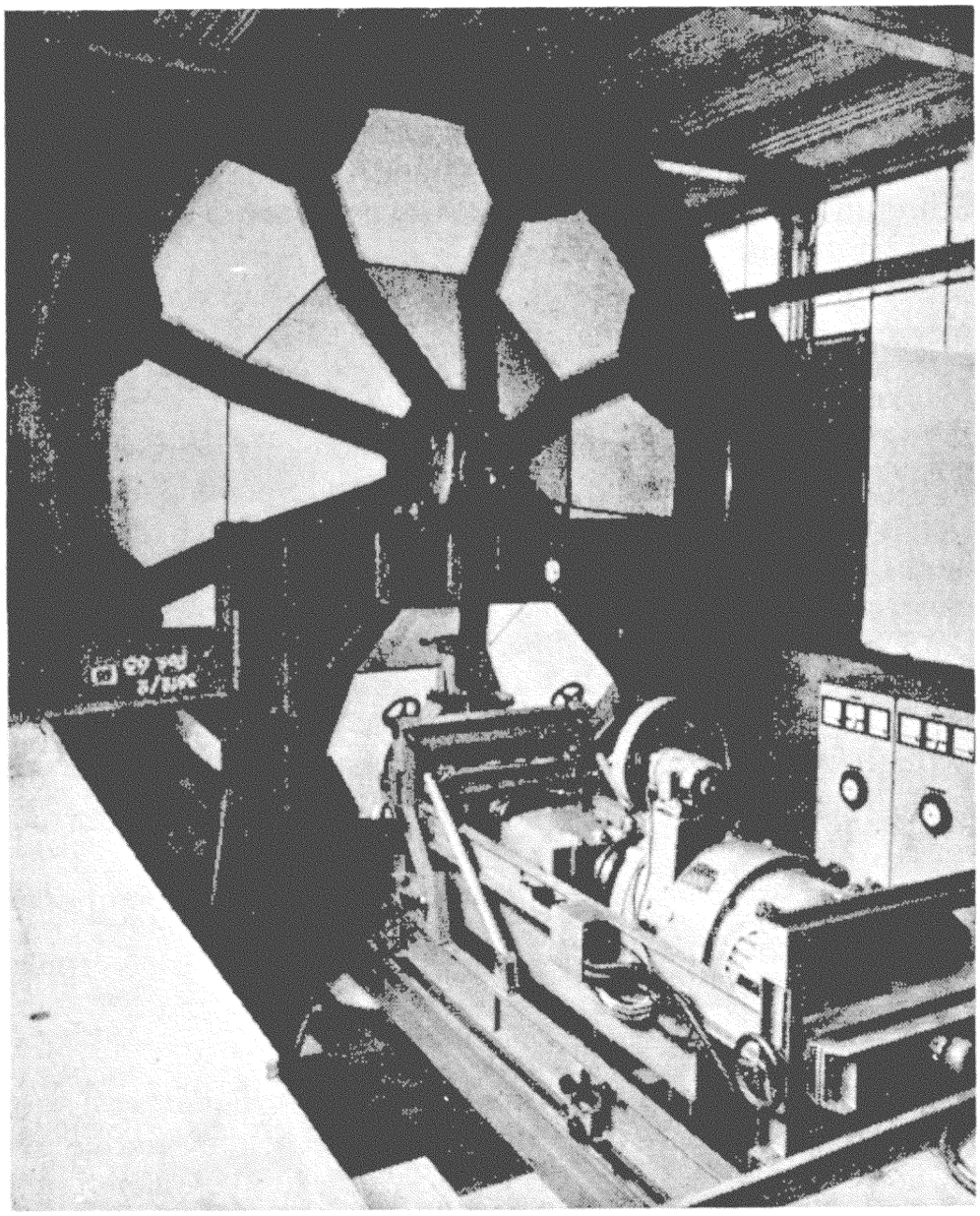

Fig. 10. Tire test bench with drum and test wheel driving system.

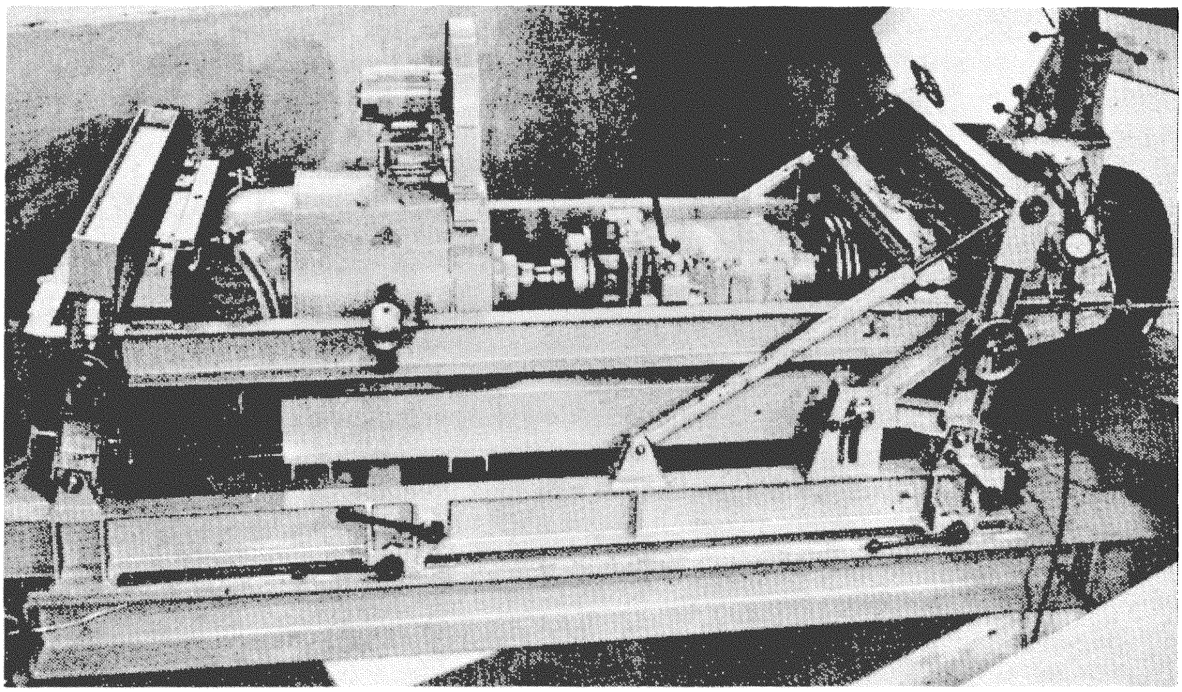

Fig. 11. Test wheel driving system. Test wheel at an angle of slip of about 25° with 10° camber angle.

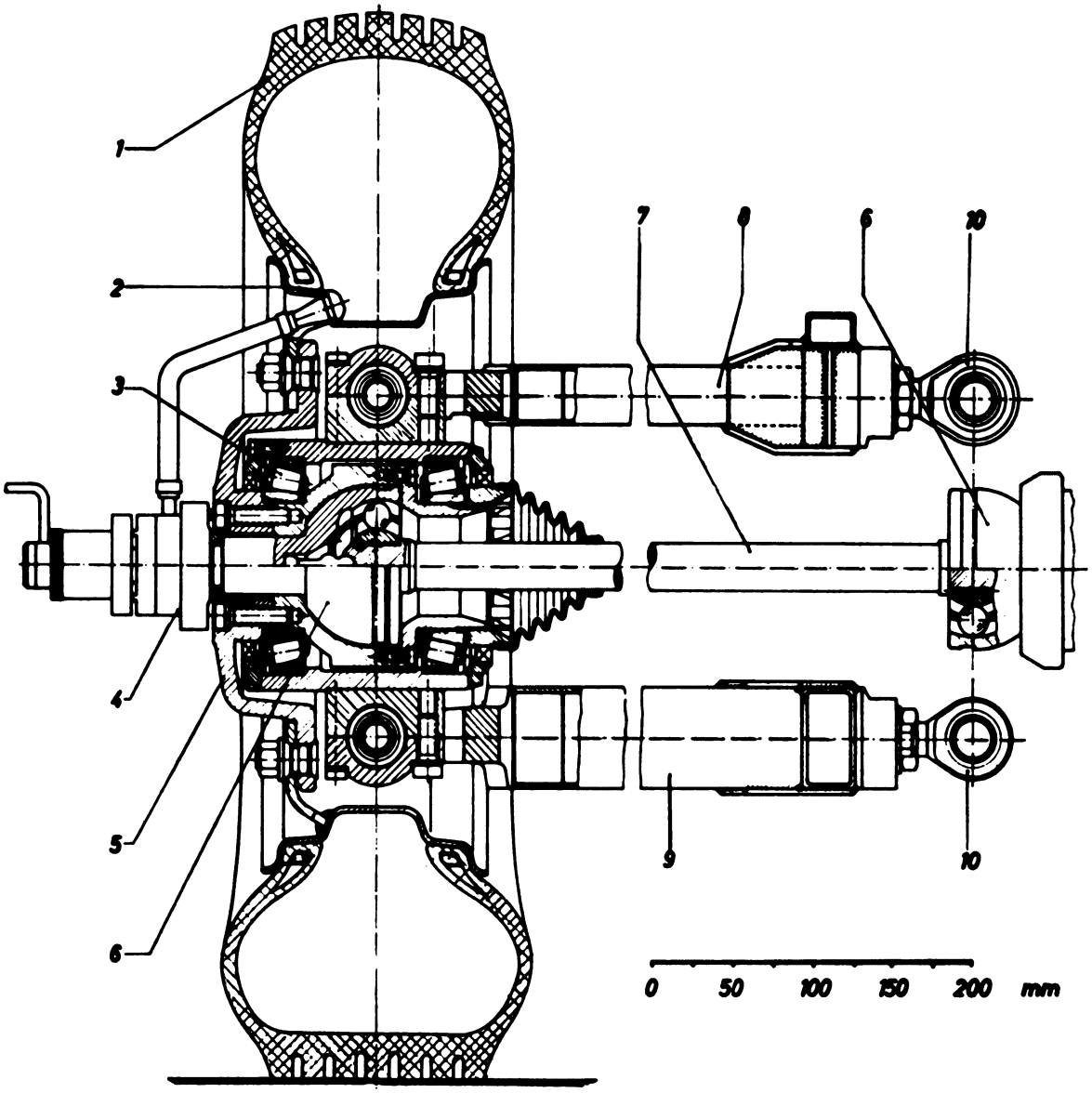

Fig. 12. Design of the suspension and hub. Further details are given in the text.

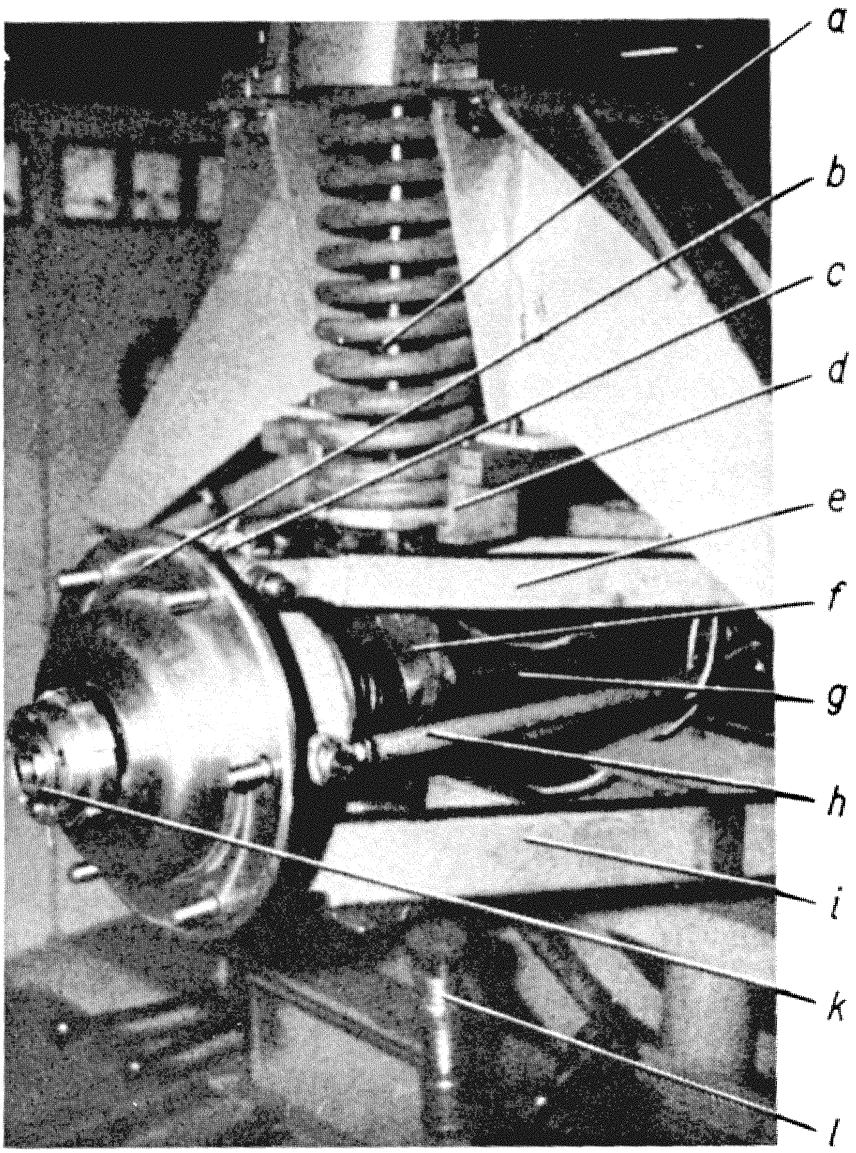

Fig. 13. Hub with suspension. (a) Load mechanism with spring and hydraulic shock absorber. (b) Hub. (c) Ball joint. (d) Force free suspension for null adjustments. (e) Upper triangular shaped steering arm. (f) Measuring element for the load. (g) Drive shaft. (h) Steering shaft. (i) Lower triangular shaped steering arm. (k) Bayonet flange for slip rings. (l) Unloading mechanism post.

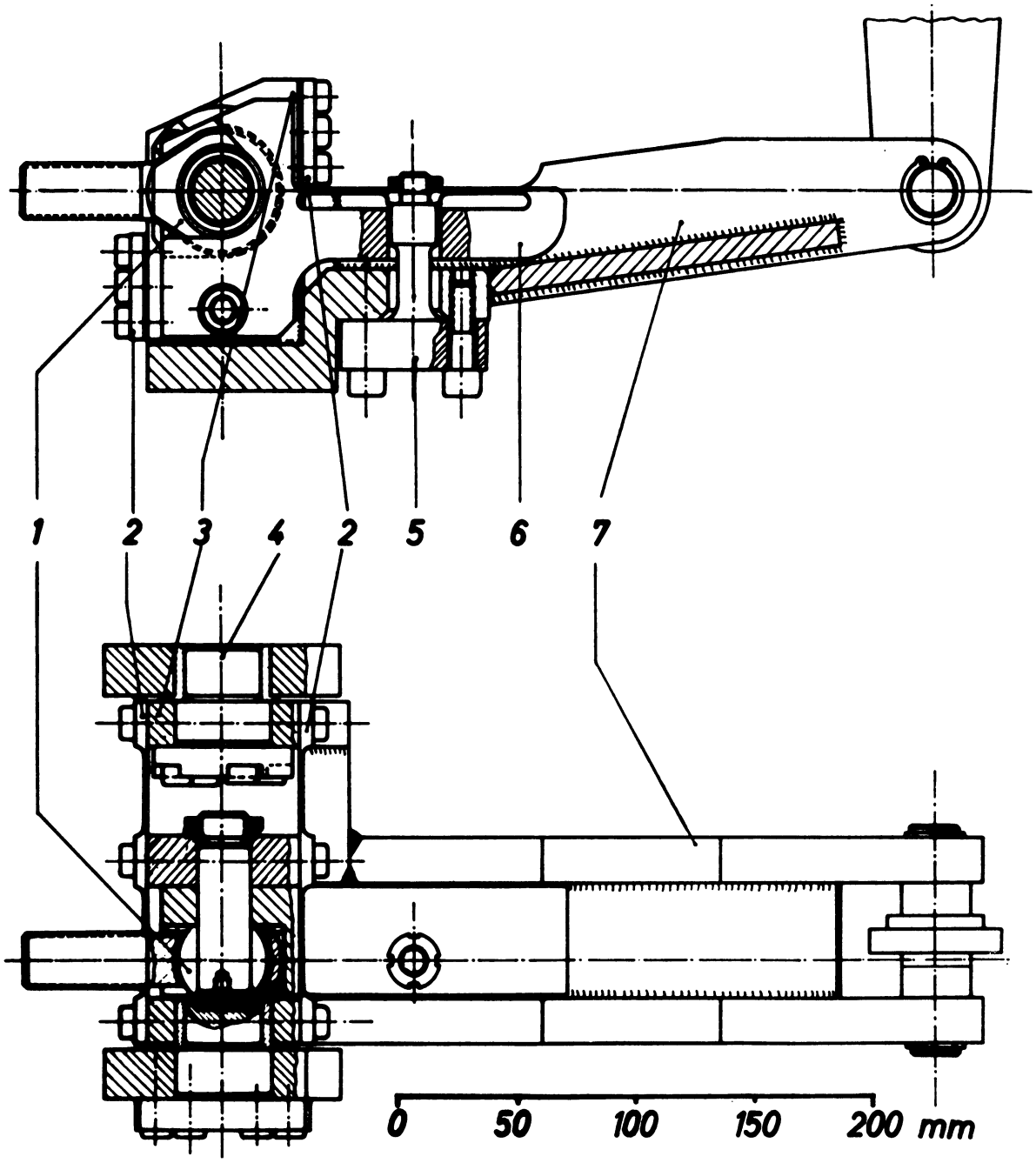

Fig. 14. Measuring system with sensor (5) and spring leaf suspension for circumferential forces and side force, as well as the friction in a camber moment. For additional explanation see the text.

flexibility was provided to allow later investigations of fast steering changes. The steering mechanism itself serves for measurement of self aligning moments.

METHODS OF MEASUREMENT

Strain gages mounted on beam and ring-shaped force transducers are used to measure forces and moments on the tire. Since only strain gages are used, a simple uniform electrical circuit was possible. All strain gages were used in the form of full bridges with temperature compensation. Data can be read directly from the bridges or can be fed into an x-y plotter, this latter method being extremely convenient during the evaluation of a tire.

Any desired combination of quantities may be chosen for the x-y coordinates. For example, one may plot:

restoring moment versus side force

side force versus circumferential force

restoring moment versus circumferential force

side force versus load

If one plots restoring moment versus side force, as first done by Gough, interpretation of the data requires a knowledge of the steer angle. During continuous adjustment of this angle, an impulse or tick controlled by a photocell at each full degree, is superimposed on the voltage of the Y coordinate, so that the x-y pen trace is interrupted by a mark.

Figure 15 is a block diagram of the measuring circuit. The voltages of the four force tranducers, labeled M1 through M4 are summed within the inverter labeled SG to give the side force and are indicated on the bridge labeled MB1. This bridge output goes through an RC element into the arm of the plotter. The output of the sensor M, giving restoring moment, goes through the bridge circuit labeled MB2 and through another RC element to the other arm of the x-y plotter.

The measuring elements for finding the circumferential and the side forces on the wheel, are situated at the four joints of the parallel triangular-shaped steering arms in the front tip frame, Figure 16. With these elements the camber moment and the frictional moment in the bearings can be determined simultaneously. The forces are transmitted from the hub onto the steering arms and then to the measuring elements. The cross-over or interaction effect of circumferential and side forces is about 0.1% for forces up to limits of the force transducer in the circumferential as well as the transverse directions. No nonlinearity was observed, so that this effect is smaller than the accuracy of the bridges used, a figure of about plus or minus 2% of full scale. Each range of the bridges was separately calibrated. No deviations from these calibrations could be observed

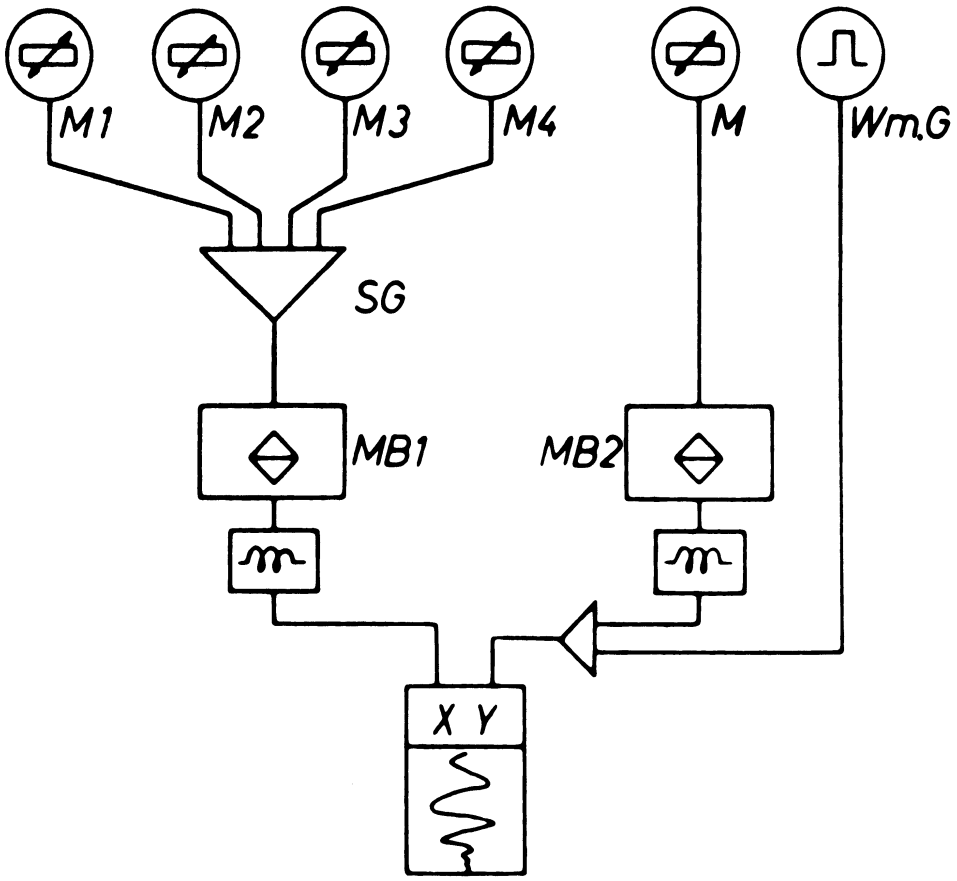

Fig. 15. Block diagram of the measuring apparatus. Restoring moment versus side forces being plotted.

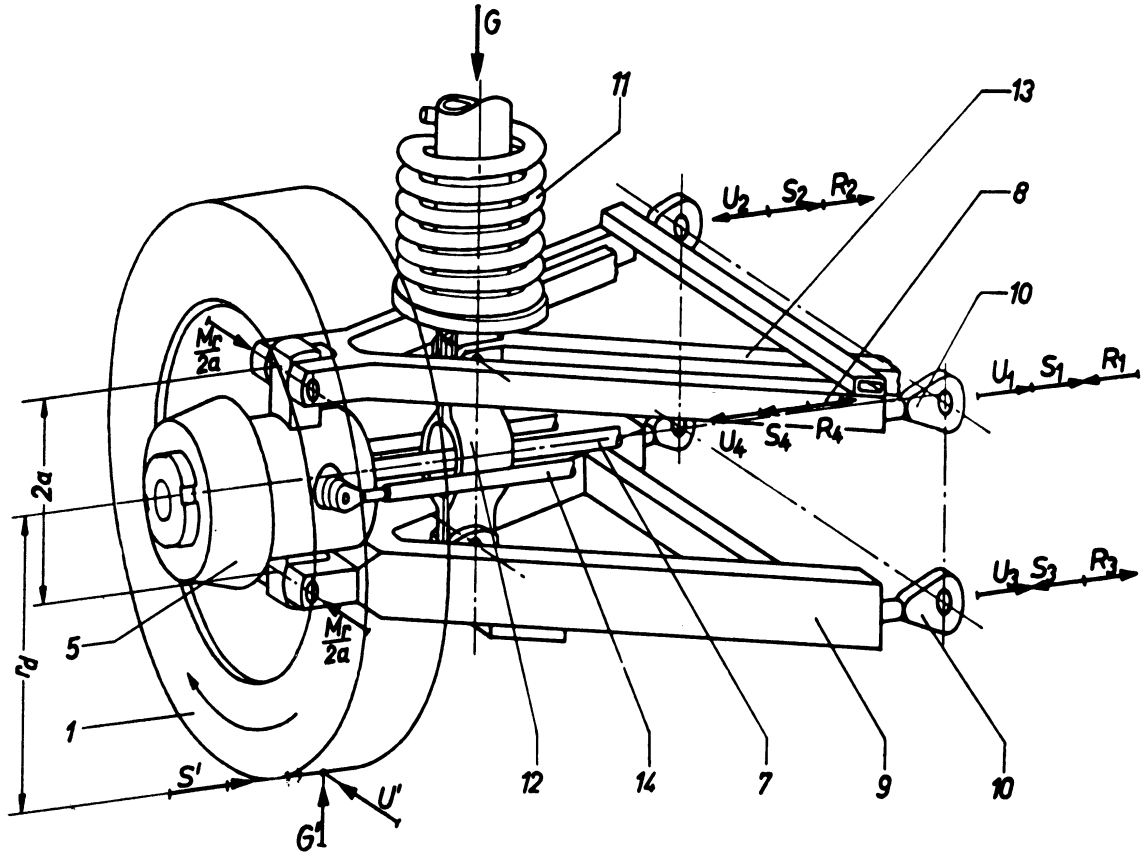

Fig. 16. Perspective view of the wheel suspension illustrating force determination on four joints of the triangular steering arms. 1. Test tire. 5. Hub. 7. Drive shaft. 8. Upper triangular steering arm. 9. Lower triangular steering arm. 10. Ball joint. 11. Loading spring. 12. Dynamometer for measuring load. 14. Steering shaft.

during later control calibrations. Null adjustment of the bridges could be obtained between experiments even with the test stand running. To accomplish this, the test wheel was unloaded using the apparatus previously described and pneumatically lifted from the track and suspended by means of a special lock. The null drift remains very small even during long test runs.

The hub is suspended in the two triangular arms and can be rotated about the vertical axis as shown in Figure 17. The moment M about this axis, the restoring moment, is supported by the two steering shafts (14) and the swinging steering arms (16). By means of this arrangement of the arms (16) the shafts absorb only the couples or couple forces resulting from the restoring moment and they are not acted upon by the axial forces from transverse or side thrust of the wheel. Restoring moment is determined by means of two ring dynamometers (15) which were built into the steering shaft. Strain gages on both dynamometer rings together form a full Wheatstone bridge. The data is displayed on a measuring bridge. The dynamometers can easily be exchanged and selected for a particular test.

The tire load acts from a spring on the dynamometer, Figure 16, and from there to the lower or triangular steering arm and thus the test wheel. A special guide maintains the ring in a vertical position. The vertical alignment is controlled by the measuring bridges such that under a load of 400 kp, in the range of highest sensitivity, no deflection is noticeable on the bridge due to circumferential and side forces. This method was much more accurate than alignment with a plumb bob and spirit level.

The force transducer is calibrated for loads acting from the tire onto the pavement. This is accomplished by letting the tire stand on a horizontal suspended plate. The calibration can be carried out using a previously calibrated load range or dynamometer. Loading of the wheel is not completely frictionless. A difference of plus or minus three percent is observed during calibration with increasing as opposed to decreasing loads.

During driving or running conditions the load approaches a mean value, due to small load changes caused by eccentricity from the tires. In all experiments, the load is accurately adjusted at the speed at which the tire is investigated.

The air pressure is measured by a manometer. It can be controlled and adjusted during running, by means of a rotating seal. All the data presented is taken with the air pressure measured after tire warm up.

Temperature of a tire is carried out by means of a set of five slip rings attached to the hub, which allows thermocouple data to be fed out of the rotating wheel system.

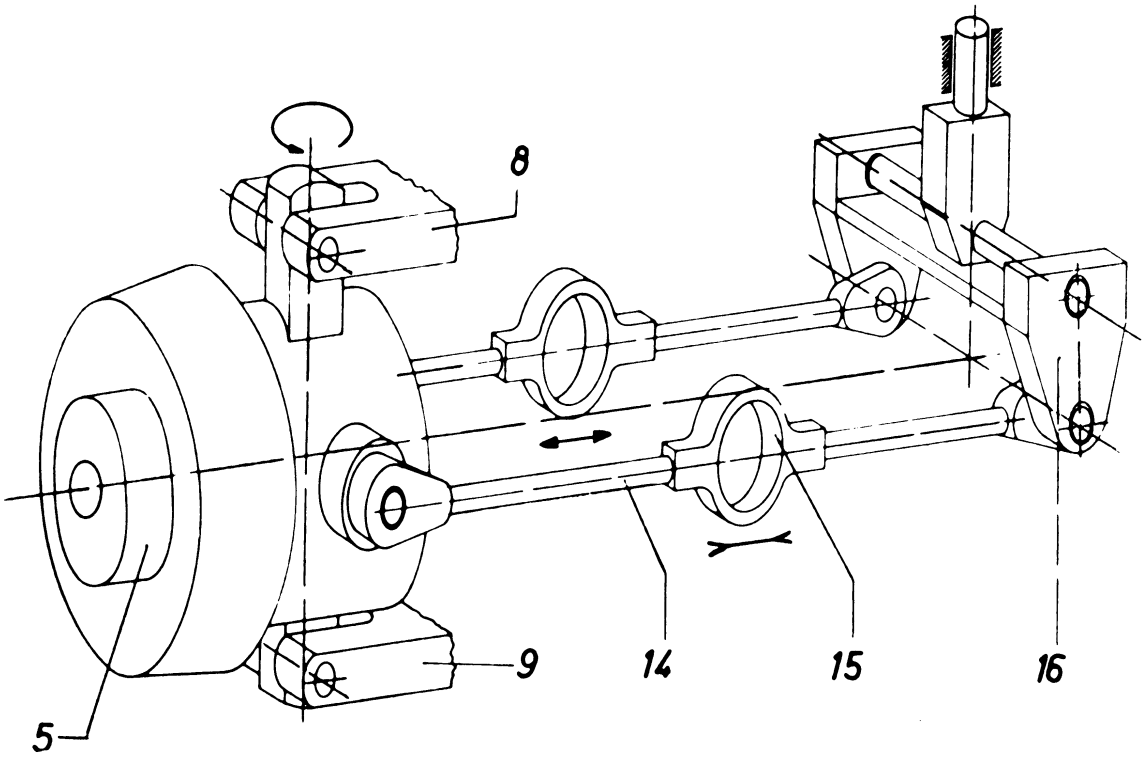

Fig. 17. Schematic view of the method for determining restoring moments. 5. Hub. 8. Upper triangular steering arm. 9. Lower triangular steering arm. 14. Steering shaft. 15. Dynamometer for the restoring moment. 16. Steering arm.

PART II

TEST RESULTS

TEST CONDITIONS

New vehicle tires have a hard external layer due to vulcanization in the mold. Initially this results in small side force values. We know that vehicles having new tires exhibit characteristics in steering, and braking which are different in the beginning than later on. The magnitude of this change, and the time required varies for all types of tires. It is especially large for tires having been stored for a long time.

The temperature of the tire also has an important influence on test results, particularly on the smooth steel surface of a test drum. For a tire started cold, we first have smaller side forces and restoring moments, and only after the tire has been running for a time, i.e., when the equilibrium temperature is reached, we obtain more or less constant values for side force and restoring moment. Figure 18 shows for three tires of different construction, and for a steer angle of $\alpha = 3°$, how side force and restoring moment change during the time of adjustment. We see that, in particular for the conventional tire which is investigated here, the magnitude of change in side force and restoring moment is considerable.

Figure 19 represents the increase in side force of a tire started cold, during six sets of measurements. These sets were recorded sequentially, by increasing the steer angle from 0° to 9°, and then decreasing it to 0° again. For the earlier sets, one can observe a marked difference between the corresponding values for increasing and decreasing steer angle.

For further investigations we now make the following assumptions:

1. For every steer angle the tire is run until its equilibrium temperature is reached. This implies that the measured values are almost constant.

or

2. The tire is run under a steer angle of 0° until heated up to the operating temperature. Then the measurements under different steer angles are taken after the tire has been running for a short time in the steered condition.

The first method cannot be applied for larger steer angles, since most tires start to become sticky after a short time. This leads to incorrect test results. Therefore, for the investigations described in here, the following procedure has been adopted: The hard external layer of the tire is removed, then the tire is run until it is warmed up to a constant temperature, under the load and inflation

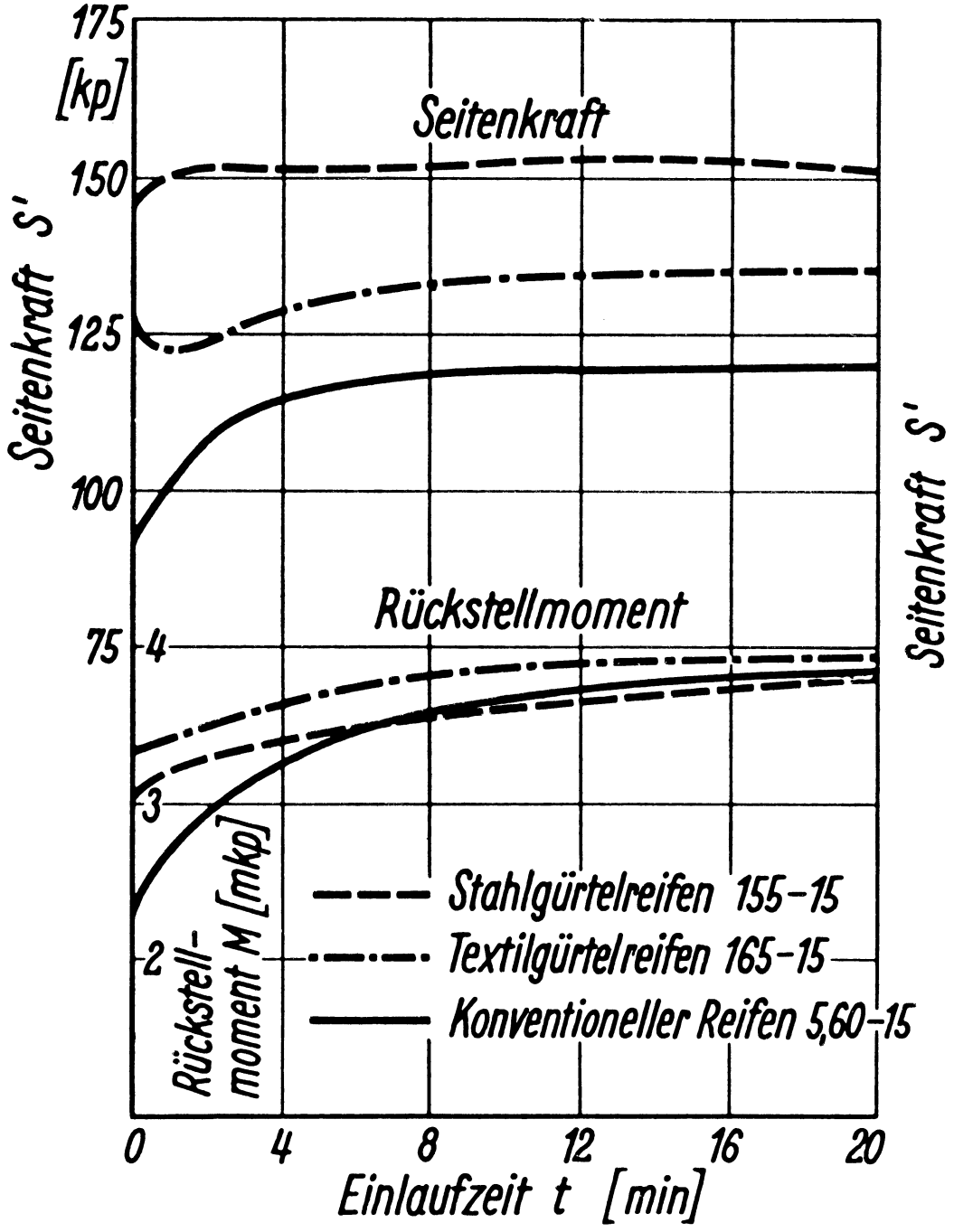

Fig. 18. Influence of running time on the side force and self-aligning moment of a new tire at 3° slip angle. Rim 4Jx15, load = 300 kiloponds, inflation pressure = 1.8 atm gage, velocity = 50 km/hr, running surface smooth.

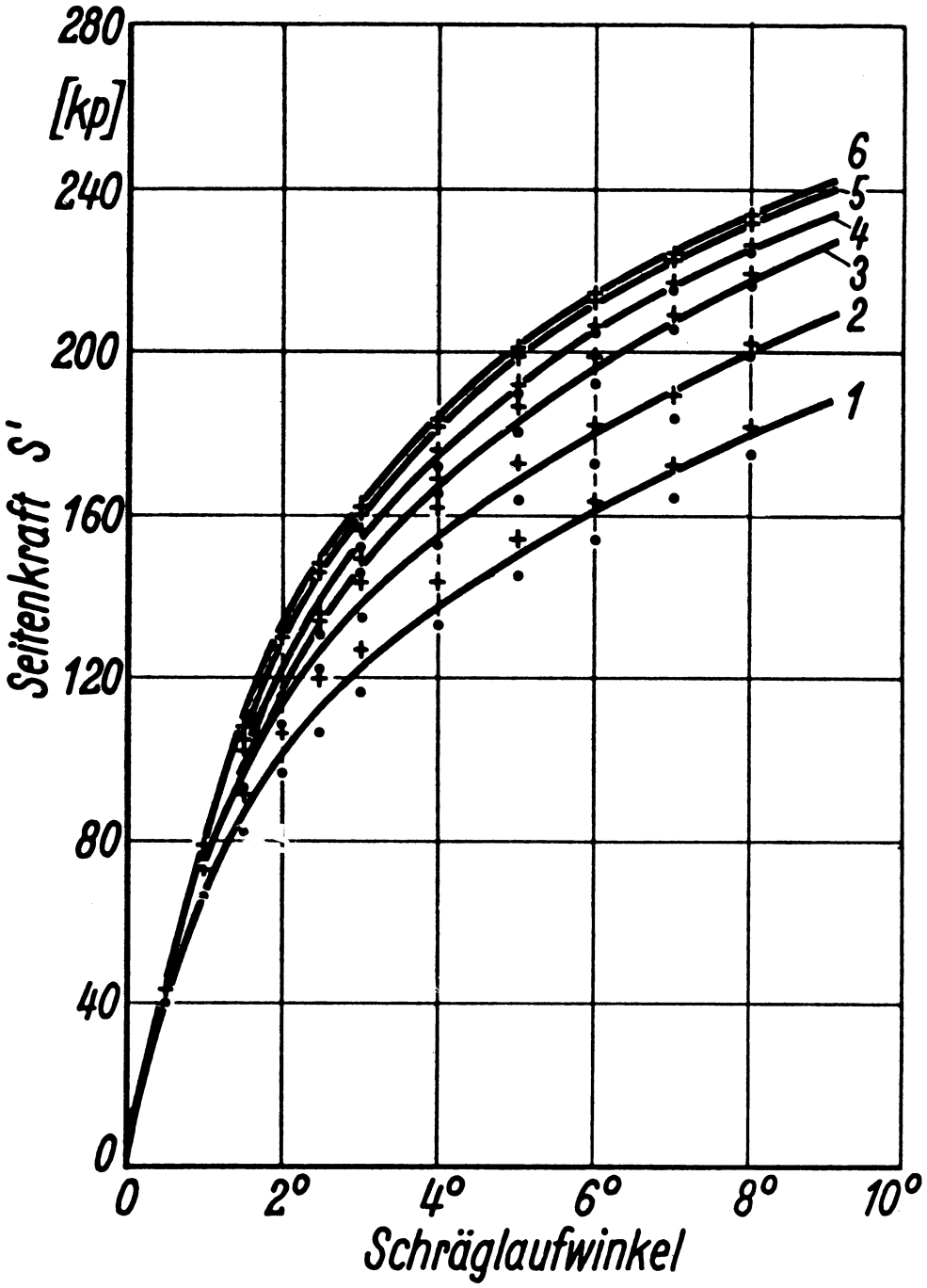

Fig. 19. Increase of side force in a new tire, not previously run, through six successive sets of measurements. Tire size 165 R 15, 100% profile, rim 4Jx15, load = 300 kiloponds, inflation pressure = 1.8 atm gage, running surface smooth.

pressure needed for the measurement but without steer angle. The conditions during the warming up time can be controlled at the bridge by observing the circumferential force, resulting from the rolling and slipping losses. These losses decrease with increasing tire temperature, and they tend toward a constant value, which is also an indication that constant operating conditions for the other measurements have been reached.

STEER ANGLE ADJUSTMENT

By means of an optical calibration device the test wheel with hub is adjusted to the geometric zero point of the steer angle, defined as parallelism between the wheel shaft and the drum shaft. A circumferential line on the drum was located by means of a light beam and the wheel was checked again. Using a measuring base of about 2.5 m, it is possible to adjust the wheel with an accuracy of $\pm$ 1/4 mm. This corresponds to an accuracy of the geometric zero point of plus or minus one minute.

It is proposed in Ref. [17] to proceed from the physical and not from the geometrical zero point for tests on vehicle tires. The physical zero point is defined as that position of the wheel under which the wheel is free from side forces. For most tires the geometric zero point does not coincide with the physical zero point. Gauss believes that this phenomenon is generated by a slightly asymmetric tread profile. The magnitude of the deviation of the physical zero point from the geometric one is determined by the amount of asymmetric wear. Deviations of up to 1.5° have been observed.

Gauss's observations can be verified. One has, however, observed in addition that in numerous cases even new tires show large deviations between the physical and geometric zero point before operation with nonzero steer angle. This was found in particular for some types of belted tires. Some tires show negative side forces at the geometric zero point. Others, however, show positive side forces. The direction of the side force at the geometric zero position could not be changed when the tire was rotated on the rim. The magnitude of the side force could be influenced only a little by this operation. From this observation, we can conclude that the fabric (construction) of a tire is responsible for its performance. This is true in particular if we have regions of asymmetric fabric, which can never be prevented completely.

Another observation which has been made for individual tire types should be mentioned here. The load was changed under constant inflation pressure. It was observed that for $\alpha = 0°$ the side force increased under increasing load. But these side forces could be decreased again when the inflation pressure was increased. We believe that for tires showing this phenomenon, the magnitude of the deflection 'f', which is also a measure for the stresses in the cord-wires, might be of importance.

The physical zero point for the side force does not always correspond to the physical zero point of the restoring moment. This has been found in part-

icular for belted tires, where for a side force S' = 0 considerable restoring moments could be observed. For example, for a load of 350 kp and an air pressure 1.8 atmospheres gauge, the values for the restoring moment were between 0.6 and 0.8 mkp. These observations have been made on a larger number of tires from the same series and they can therefore not be purely accidental (random). This must be a basic characteristic for this type of tire, one which is influenced by the construction or manufacturing process.

This characteristic with respect to the restoring moment could not be observed for tires of the same type, but from a later series. Since the construction of this type of tire has not been changed, we must assume that this is a question of how the tire is manufactured. This observation is illuminating insofar as it indicates that the performance of a tire is not only a function of its construction, but also of the manufacturing. One of the reasons might be that the belt or band is not symmetric about the center plane of the tire, or that the orientation of the belt is oblique and thus makes one believe that the camber has been changed.

Finally, the following reasons were of importance for the decision to refer the steer angles to the geometric zero position:

1. The behavior of the side force in the geometric zero position is in many cases a property of the tires, which has its history in the construction or in the techniques of manufacturing.

2. For a number of tires the physical zero position of the side force is not equal to the physical zero position of the restoring moment.

3. The design of vehicle tires is in general governed by geometrical aspects.

INVESTIGATIONS ON CAR TIRES

The reproducibility on the new test stand was tested by detailed preliminary studies. It was possible, by an extensive series of measurements, to obtain a survey of the scatter within the sets of different tire types. Special attention was paid to the influence of drum curvature when comparing measurements made on drums with external tracks and on drums with internal tracks. By performing steer angle investigations on a smooth drum surface, the values measured here could be compared with values measured on other test stands. It was found that the influence of steer angle, camber, load and air pressure on the tire characteristics is of the same tendency as for test stands with an external track. The values for the side force, however, are in general higher on the internal track.

INFLUENCE OF THE TRACK SURFACE

The adjustment mechanism described in Part I, causes a continuous change in steer angle with an angular velocity of 0.4°/second. This means the traveling

time for a measuring curve from 0 to 10° is 25 seconds. At the same time the measured values can be recorded by a X-Y plotter. Although the measuring time is relatively small, the rolling surface (contact surface) of most tires becomes sticky for larger steer angles, even under small loads. The results from measurements performed on a conventional tire shown in Figure 20 (reproduction of the original, reduced in scale) show the problems arising when determining the map of tire characteristics on a smooth steel surface.

The map of tire characteristics becomes much clearer if, after Gough, the tire tests are performed on a rough surface. The difference in the trend of the characteristics can be seen from the results presented in Figure 21, which were obtained from a conventional tire on a corundum surface of grain size K80. The values for the side force are higher for the finer grain size than for the coarse one. The values for the restoring moment vary only little for both grain sizes.

The increase in restoring moment on the corundum surface compared to the smooth steel surface, however, is considerable. This observation has been made for all comparative tests.

The influences of the track surface on the steer angle characteristics is basically the same for belted tires, as for conventional tires. The magnitude of the influence, however, varies.

Within the range of steer angles of 0 to 9°, the observations pertaining to the influence of the track surface can be summarized as follows:

1. The side force as well as the restoring moment are larger on a corundum surface than on a smooth steel drum surface for all types of tires. But this is only true if we omit all measurements from tires whose tread surface had become sticky before the measurement was made.

2. The side force is larger on the corundum surface with fine grain, than on the one with coarse grain. The difference in the values, however, is small.

3. No trend is apparent for variation of restoring moment with grain size. In general the differences are small.

4. The drum surface has almost no influence for steer angles up to 2°; however, at 4° the influence can be quite considerable.

5. The order of classification with respect to the steer angle behavior may change when we go from the smooth steel surface to the corundum surface, especially for larger steer angles. This, however, has not been observed if the results obtained from the corundum surface with different grain size were compared.

6. The influence of the tire temperature on the test results is smaller for investigations made on the corundum surface than on the smooth steel surface.

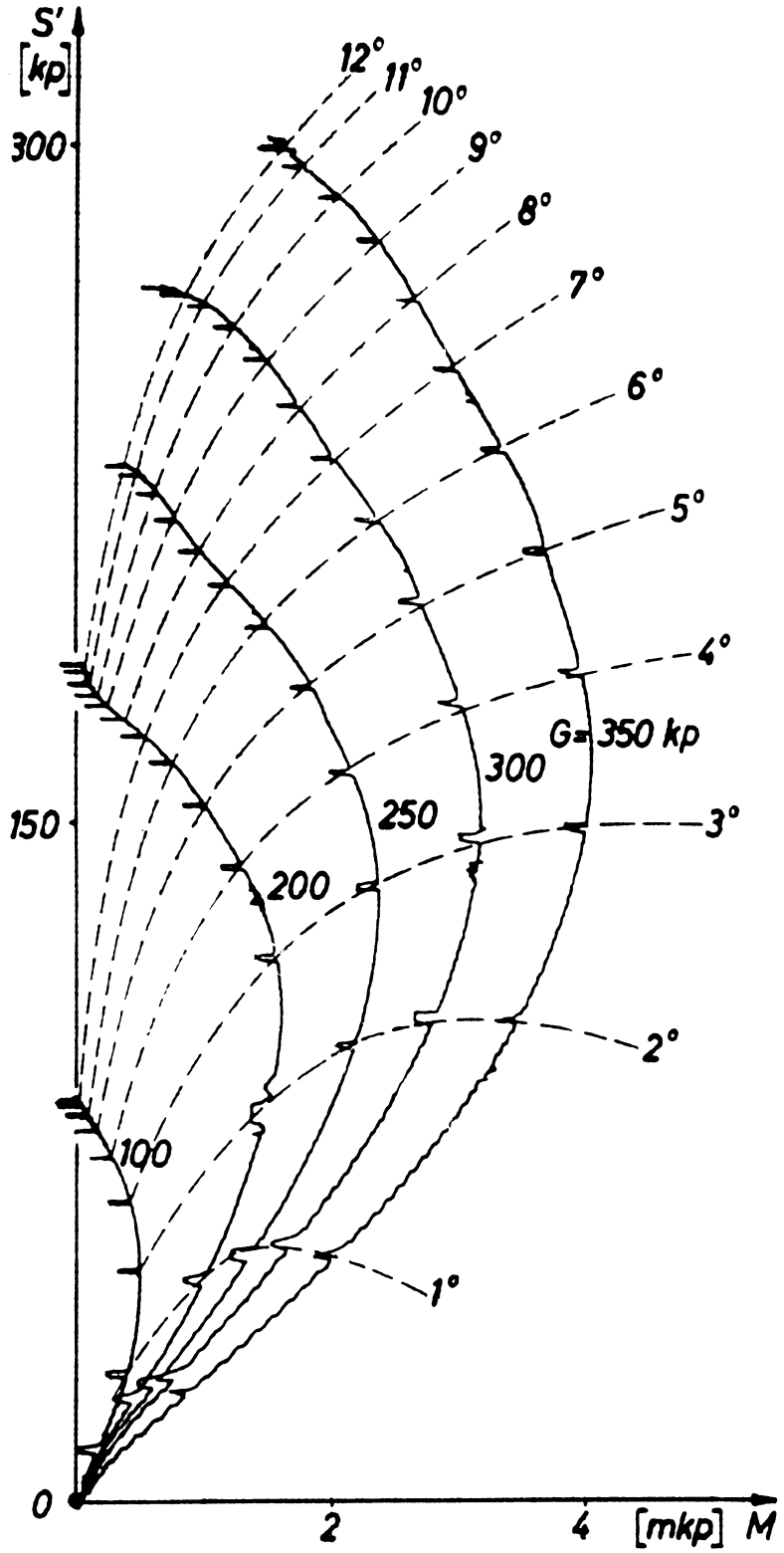

Fig. 20. Map of tire characteristics (after Gough) for a smooth steel surface (reduced reproduction of the original). Tire 6.00-15, profile 100%, rim 4x15, p = 1.8 atu, V = 50 km/h.

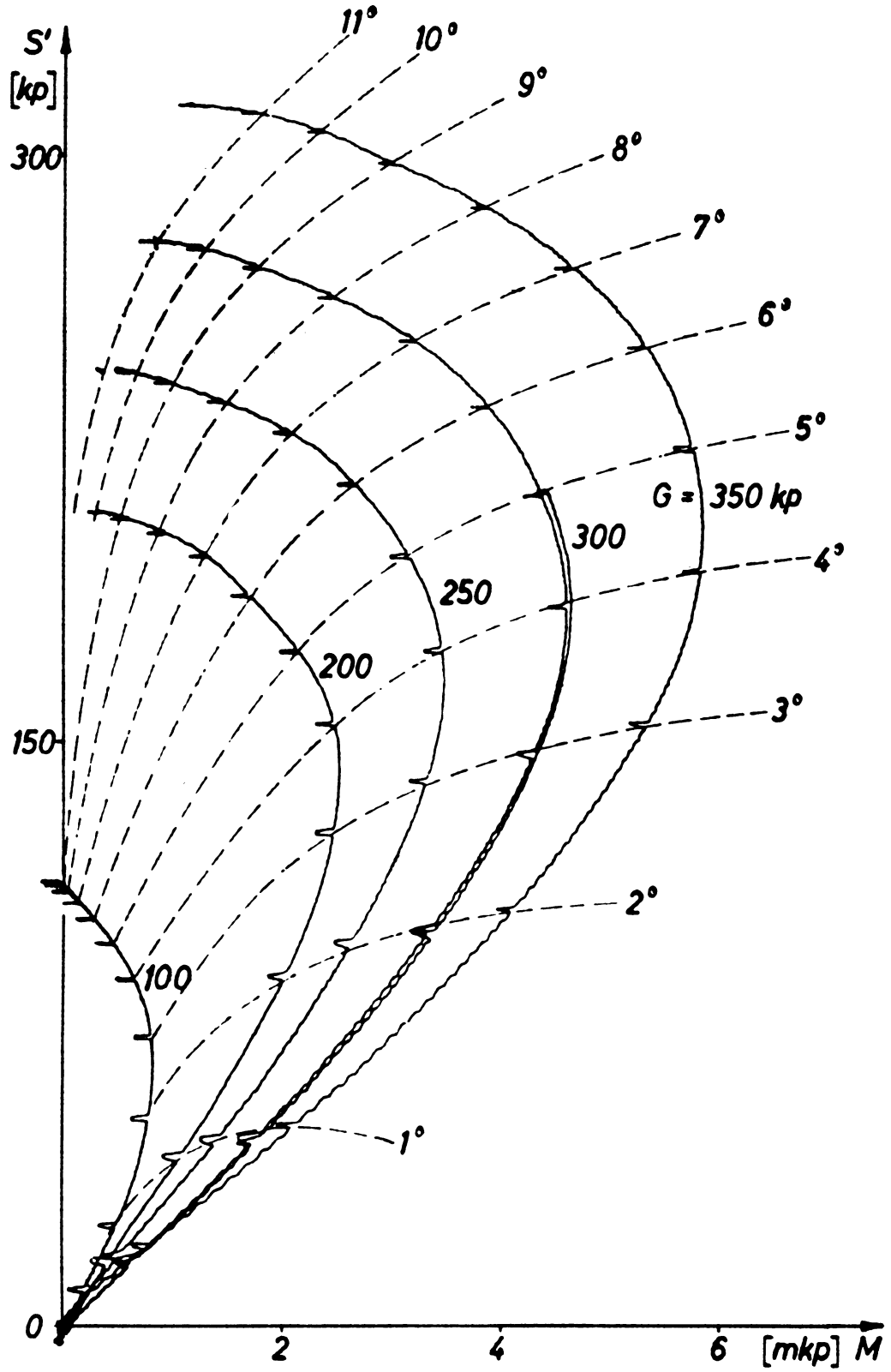

Fig. 21. Map of tire characteristics of a conventional tire 6.00-15 on a corundum surface. Grain size K 80 (reduced reproduction of the original), profile 90% to 100%. The other data are the same as in Fig. 20.

INFLUENCE OF THE CONDITION OF THE PROFILE (TREAD)

It has been observed over and over again that the condition of the profile has a considerable influence on the characteristics of a tire. For the series of measurements performed on a corundum surface, the tire wear increases, particularly for larger steer angles. It was found that a comparison between the maps of tire characteristics is possible only if the profile condition is also given. Therefore several tires of different construction were investigated for different profile conditions. The degree of wear was defined as:

$$\text{Profile condition} = \frac{h}{h_o} \cdot 100\%$$

h_o is the profile depth of the new tire and h is the profile depth of the test tire. Due to the irregular wear along the tire circumference, the profile depth at the center was measured at 4 to 8 equally distributed locations. Then the average was taken from these values. The information given for the profile condition refers to the profile at the beginning of any series of measurement (Figure 22).

For every steer angle a gradually increasing side force can be observed with decreasing profile. The influence of the profile condition on the change in side force (cornering force) first increases with increasing steer angle, then it decreases again for larger steer angles. This observation and the fact that for large steer angles, the change in profile condition has little effect on the restoring moment are true for all tires inveatigated.

Figure 23 shows the side force increase per 1 mm wear ($\Delta S'/mm$) as a function of the steer angle with different wheel loads as a parameter.

Each of these curves shows a maximum for a certain steer angle. The smaller the load, the smaller the steer angle for which the maximum is reached. We also notice that the increase in side force due to wear is not proportional to the load, but is relatively larger for small wheel loads. This can be seen clearly from Figure 24 where increase in side force due to profile wear is related to the side force for a new tire. For a steer angle of 2°, the increase in side force for 100% of profile wear (0% condition) is about 40% compared to a new tire for a load of 300 kp. For a load of 100 kp the increase is almost 90%. Large steer angles, however, change this tendency completely. Thus for $\alpha = 9°$, the corresponding values for the increase in side force are 15.5% for 300 kp, and 11.5% for 100 kp of wheel load.

The steer angle characteristics of a tire are greatly influenced by its profile condition. Thus, it is necessary to know the profile condition in order to judge a tire's characteristics.

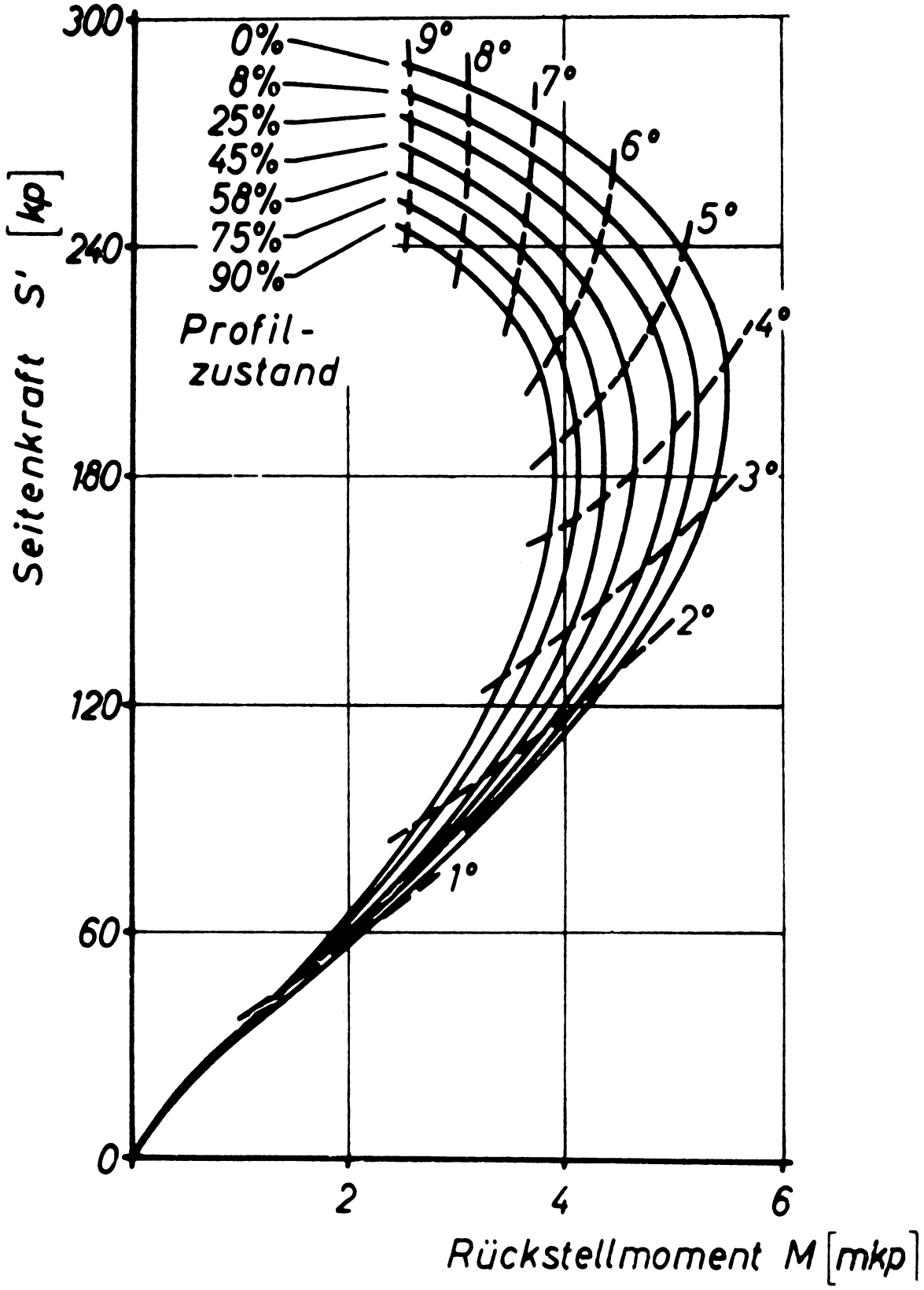

Fig. 22. Map of tire characteristics as a function of different profile (tread) conditions. Tire 5.60-15, p = 1.8 atu, rim 4Jx15, V = 50 km/h, G = 300 kg, surface K 80.

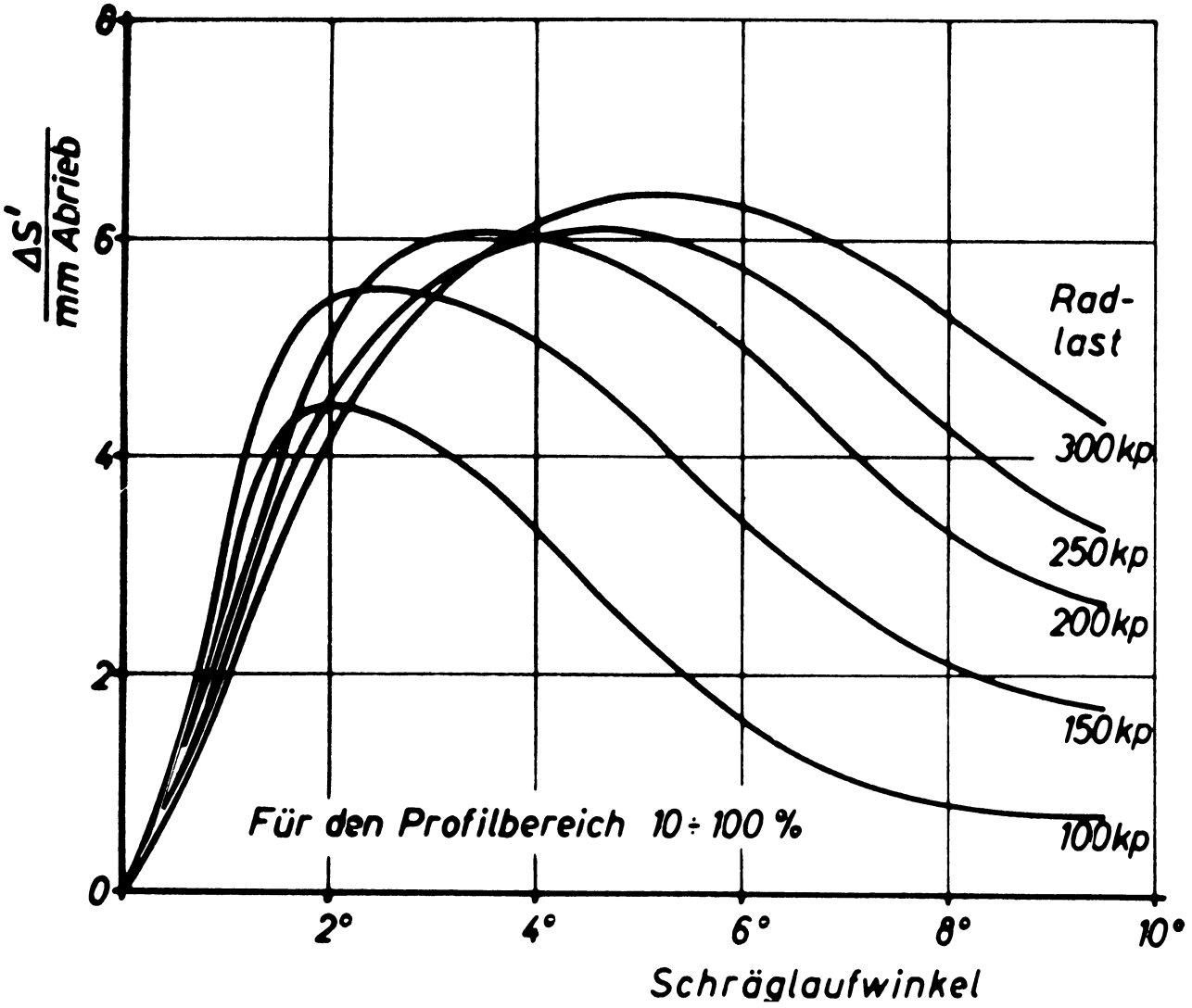

Fig. 23. The increase in side force per millimeter wear under various wheel loads as a function of the steer angle. Tire 5.60-15, rim 4Jx15, p = 1.8 atu, V = 50 km/h, surface K 80.

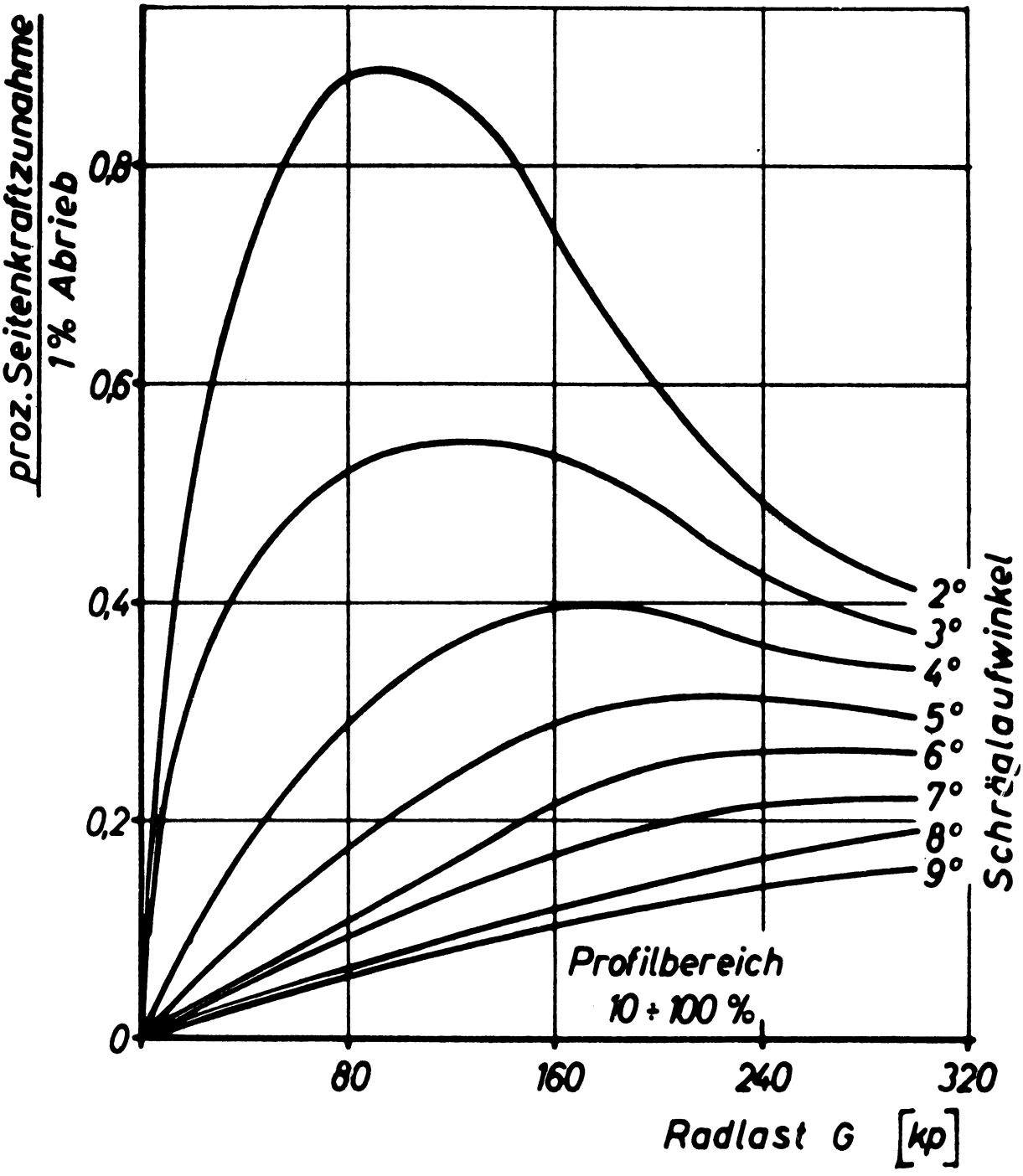

Fig. 24. The percentage change in side force increase per percent tire wear as a function of steer angle α and the load G.

The maximum circumferential force which can be transmitted by a vehicle tire depends on the coefficient of friction between the tire and the pavement, and also on the magnitude of the wheel load. The coefficient of friction not only depends on the quality (condition) of the tire, and the pavement, but also on the speed [5], the contact area pressure and the temperature [36]. We define two kinds of friction coefficients:

1. The static coefficient of friction $\mu_h = \frac{U_{max}}{G}$

2. The dynamic coefficient of friction $\mu_y = \frac{U_s(100\%)}{G}$

Therefore, the static coefficient of friction is the ratio between the highest possible circumferential force, that can be transmitted and the corresponding wheel load. The dynamic coefficient of friction is in general given for 100% slip. For all tires investigated on the test stand, the dynamic coefficients were smaller than the static coefficients. However, the ratio μ_y/μ_h is different for each pair of tire and pavement values. For some tires, measurements of the side force under right hand and left hand steer angle gave different values. Similarly, it was observed that for some tires the measurements of the circumferential force were dependent on the sense of rotation of the tire. For most tires the scatter in the circumferential force was small for both directions of rotation. The obvious supposition that the larger deviations result from profile (tread) effects could not be verified, because sometimes profiles which were symmetric with respect to their circumference, were dependent on the sense of rotation whereas for asymmetric profiles no influence of the sense of rotation could be observed.

For all cases, however, the maximum circumferential force was larger for traction than for braking. The deformations due to circumferential forces on a wheel at rest are symmetric in both directions. They are independent of the direction. This idea, however, cannot be used for the wheel under traction and braking. Under traction the contact patch of the tire is reduced in area, before entering the contact region and extended when leaving it. For braking this effect is the other way around. [5, 22] But since, according to Koesster and Hey [5,22], the resultant of the pressures in the contact area does not coincide with the center of the contact area for both cases, the deformations in a rolling tire are not symmetric with respect to the direction of the circumferential force. The effect on tire behavior can be observed on the test stand.

With increasing tractive force the rolling radius of the tire increases slightly, while decreasing with increasing braking force. This gives rise to the idea that the tire under tractive force, makes contact through the bulge of the tread caused by shrinkage before entering the contact area. By this process the wheel axle is raised slightly. Under braking, however, the tread and the carcass of the tire are slightly indented, due to dilatation before entering the contact area. This implies a decrease in the rolling radius of the tire.

Tires with worn tread can transmit higher circumferential forces on a dry

pavement than new tires; however, the influence of the tread on the circumferential force is smaller than on the side force.

No uniform tendency can be found in the effect of the air pressure on the maximum transmissible circumferential forces, Figure 25. For very small air pressures (less than 1 atmosphere gage), the transmitted circumferential force increases with increasing air pressure. For some conventional tires, the increase continues up to air pressures of 4 atmospheres gage (see Fig. 25 at the top). The difference between the circumferential forces for traction (+ U), and for braking (- U) is only slightly effected by the inflation pressure. On the other hand, the belted tire 165 R 15, shown at the bottom of Fig. 25, reaches a maximum for the circumferential forces at an air pressure between 1.5 and 2 atmospheres gage. Air pressure influences the maximum traction and braking forces in a similar way. The maximum circumferential force is in general, larger for traction than for braking.

THE TIRE UNDER CIRCUMFERENTIAL AND SIDE FORCE

There are only a few measurements available on the influence of the circumferential force on the side force. The work from Tschundukow [50] mentioned earlier investigates a tire under the influence of braking forces. The measurements obtained point-by-point and their scatter do not allow any extensive survey, particularly near the limit of adhesion. Bergman's and Freeman's measurements do not reach the limit of adhesion for a tire studied under traction. In addition, it seems that both results contradict each other within the range of small circumferential forces. Bergman's measured curves do not have a horizontal tangent for zero circumferential force, and steer angle of more than 1°, but have a considerable slope. We therefore must conclude that in the range of small braking forces, the curves still increase, which verifies Gauss's observation that for small braking forces the side forces increase at first. On the other hand, Tschundukow believes that for a certain steer angle of the wheel the side force remains constant under variations of the circumferential force (braking force), and that it starts decreasing only at a certain magnitude of the circumferential force. The reproduction of the original data, reduced in scale, (Figures 26 and 27) confirms both observations. The behavior of the side force investigated in Fig. 26 for a conventional tire is typical for this kind of tire construction; i.e., a relatively large decrease of the side force under tractive forces - U, at the beginning A typical observation for this tire, is that with increasing tractive forces, the side force does not decrease linearly for small steer angles as is the case for most conventional tires.

A number of these tire types have been investigated on different pavement surfaces, under various tread conditions and wheel loads. Except for the absolute magnitude of these measurements, nothing changed in the characteristic picture of this tire. Tires of same type of construction, but from different manufacturers show a similar behavior, but one can notice after a few sets of measurements that each tire type has its own individual characteristics. For belted tires

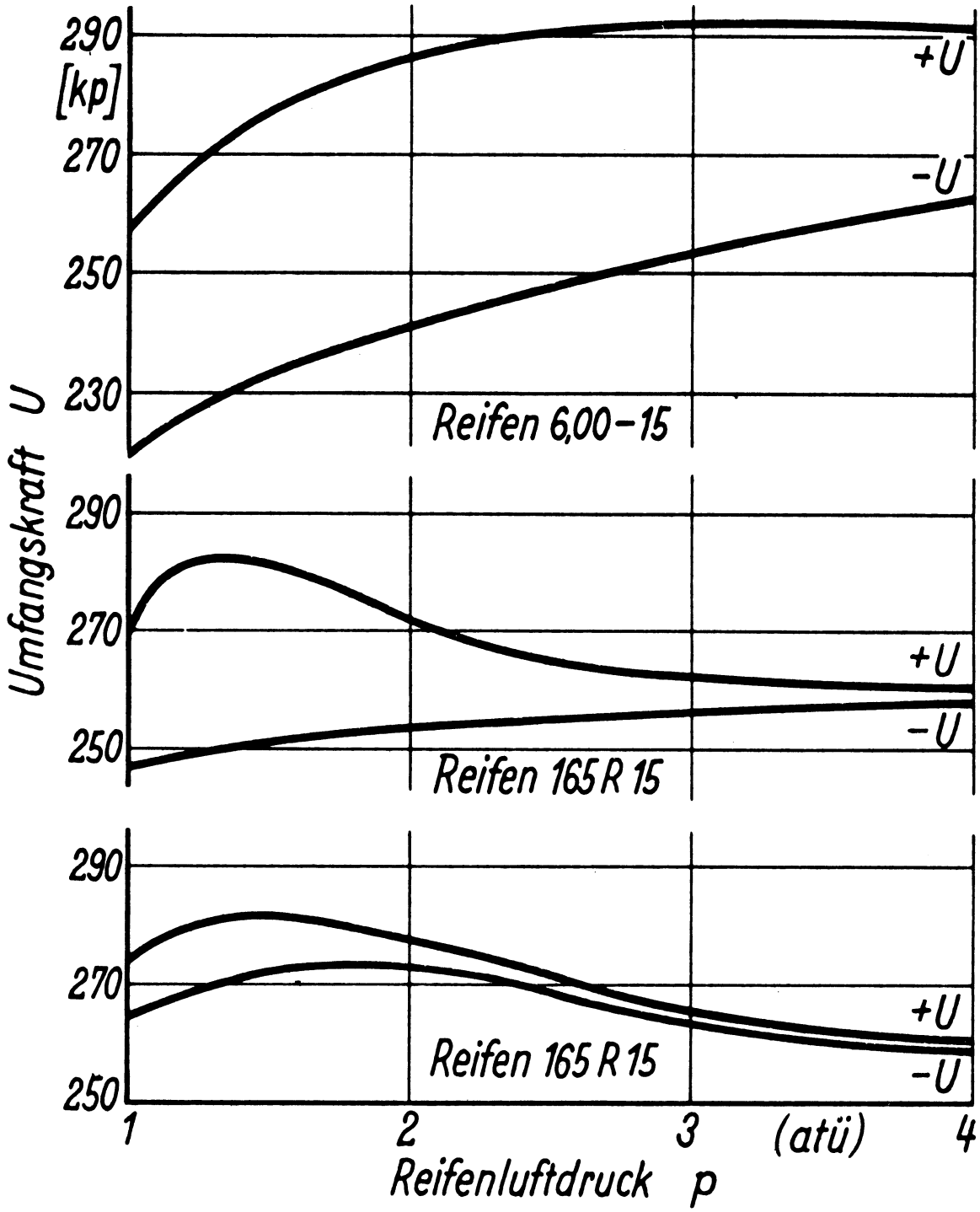

Fig. 25. The influence of the air pressure on the circumferential force for traction and braking for three tires of different construction. Profile 60%-90%, rim 4Jx15, G = 250 kg, V = 50 km/h, surface K 80.

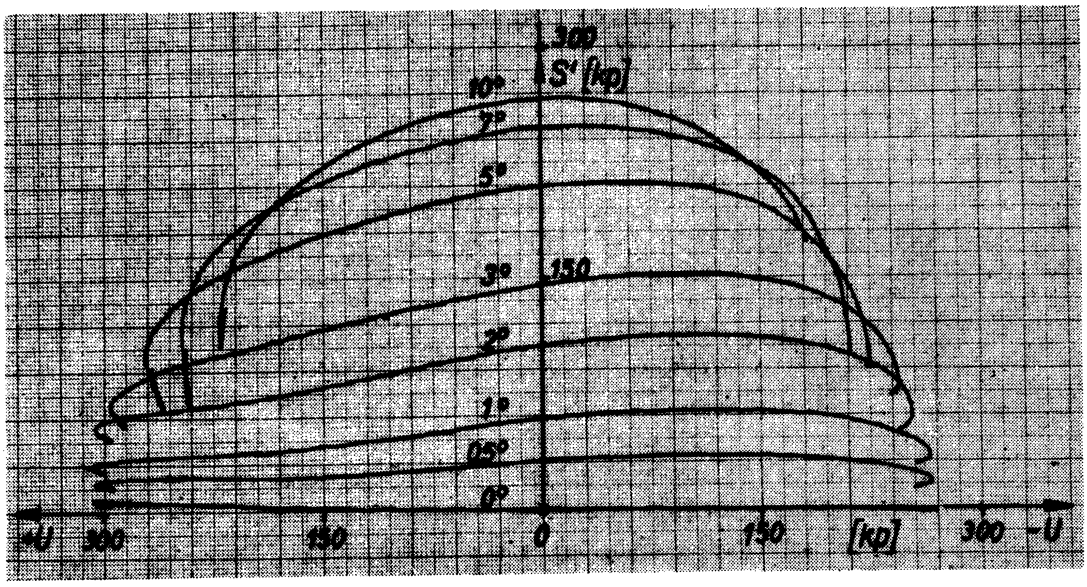

Fig. 26. The side force S' as a function of tractive force (+U) and braking force (-U) for different steer angles. Tire 6.00-15, profile 100%, rum 4Jx15, G = 300 kg, p = 1.8 atu, V = 50 km/h.

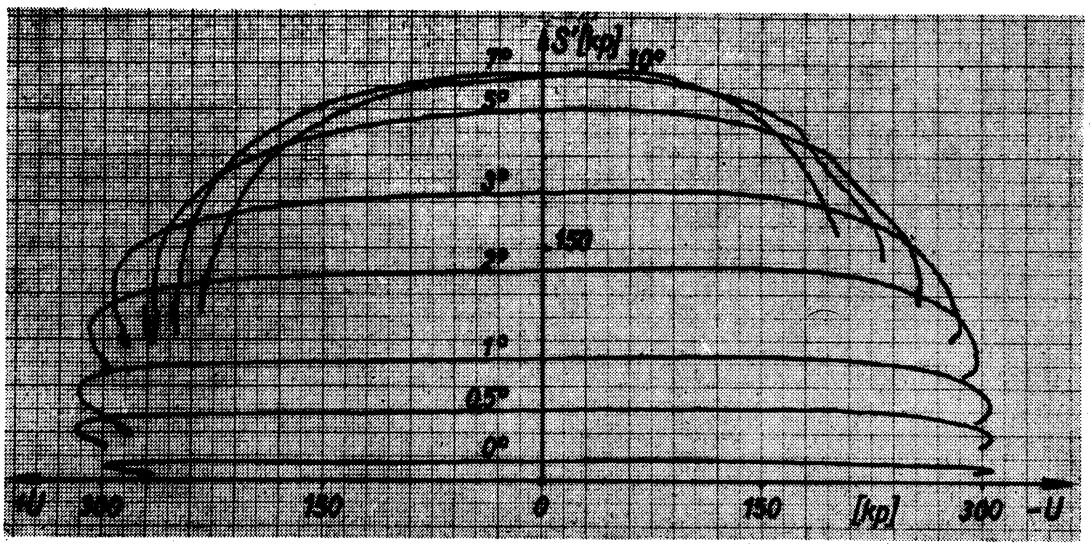

Fig. 27 The side force S' as a function of the tractive force (+U) and braking force (-U) for different steer angles, belt tire 165R-15, profile 60%. All other data same as in Fig. 26.

(see Fig. 27) the decrease in side force under traction and the increase under braking is much less. Judging this tire on a basis of individual measurements might give rise to the idea, that small circumferential forces have no influence on the side forces. All of the new tires in this series had a positive side force for $\alpha = 0°$.

The results from another belted tire (Fig. 28) which had heavy one-sided wear show that, due to the irregular tread, the characteristic picture can change completely. This type of tire also shows a similar tendency to the tires in Fig. 27, if it is worn.

According to Bergman [1] the combination of the side force, and the circumferential force leads to a change in the spring rate in the direction of the side force. It we consider the displacements of an area element ΔF in the contact area under a non-zero steer angle, and under the influence of the circumferential force, we find that the observed change in spring rate is only due to the effects of additional stresses in the contact area caused by the circumferential force.

The processes in the contact area are complicated but they can be simplified (Fig. 29). Let the direction of the drum track be from A to B. The tire runs under a steer angle α. AC is the meridian of the tire for which the area element ΔF just touches the track in A. Under the effect of steer angle the area element is carried along by the track and is deflected more and more from its tire meridian. If it has reached, for example, point S_1, then the distance OS_1 is equal to the amount of deflection of the area element ΔF due to steer angle. Under a braking force without steer angle, the area element would be deflected by the distance OU_B, and under tractive force by OU_A. These considerations are based on the assumption of no slip in the contact area, and therefore the area element can move only along the line A-B. The resultant displacement of OS_1, and OU_B corresponds to the distance OR_B. The partial side force on the tire due to ΔF is then, for braking, $\Delta S_B = C_S \cdot U_B R_B$ and for traction $\Delta S_A = C_S \cdot U_A R_A$. Hence ΔS_B is $C_S \cdot OU_B \alpha$ times greater and ΔS_A is $C_S \cdot OU_A \alpha$ smaller than ΔS, the partial side force without circumferential force. With increasing circumferential force, and also for large steer angles we will have slip in the contact area, which is superimposed more and more on to the displacements, and slip caused by pure deformation while running.

For tires with a small slip due to circumferential deformation, the difference in the distances $U_B R_B$ and $U_A R_A$ respectively is also smaller and therefore the influence of the circumferential force on the side force is less. For belted tires compared to conventional tires, the ratio of slip due to deformation while running is about 1:3.

Near the limit of adhesion the following conclusions are based on a great number of measurements:

1. Side force and circumferential force influence each other.

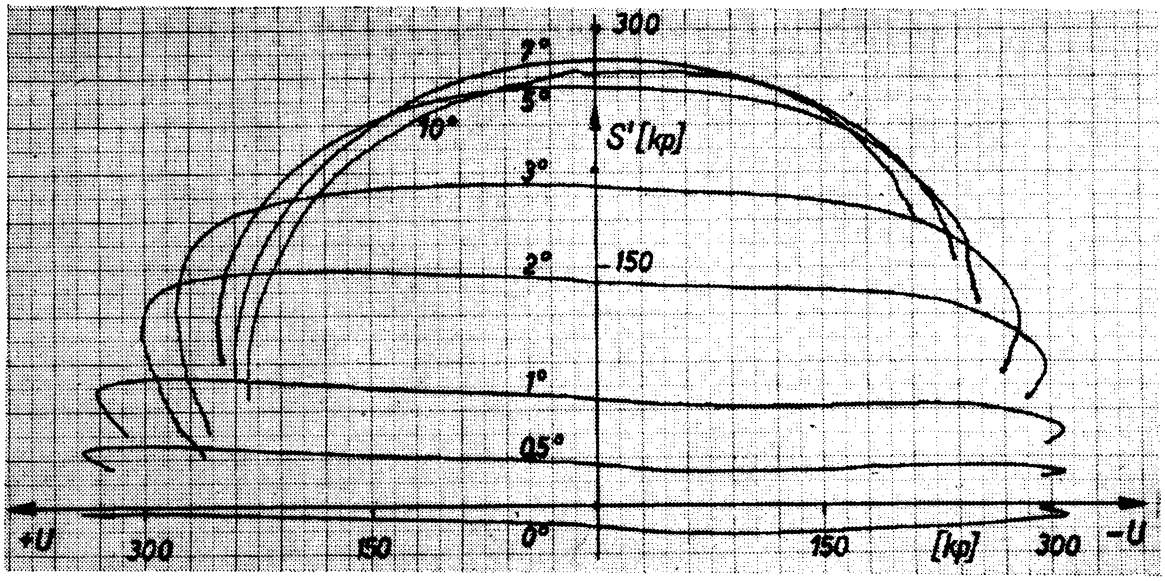

Fig. 28. The side force S' as a function of tractive forces (+U) and braking force (-U) for different steer angles. Belted tire 165R-15, profile 30%. All other data same as in Fig. 26.

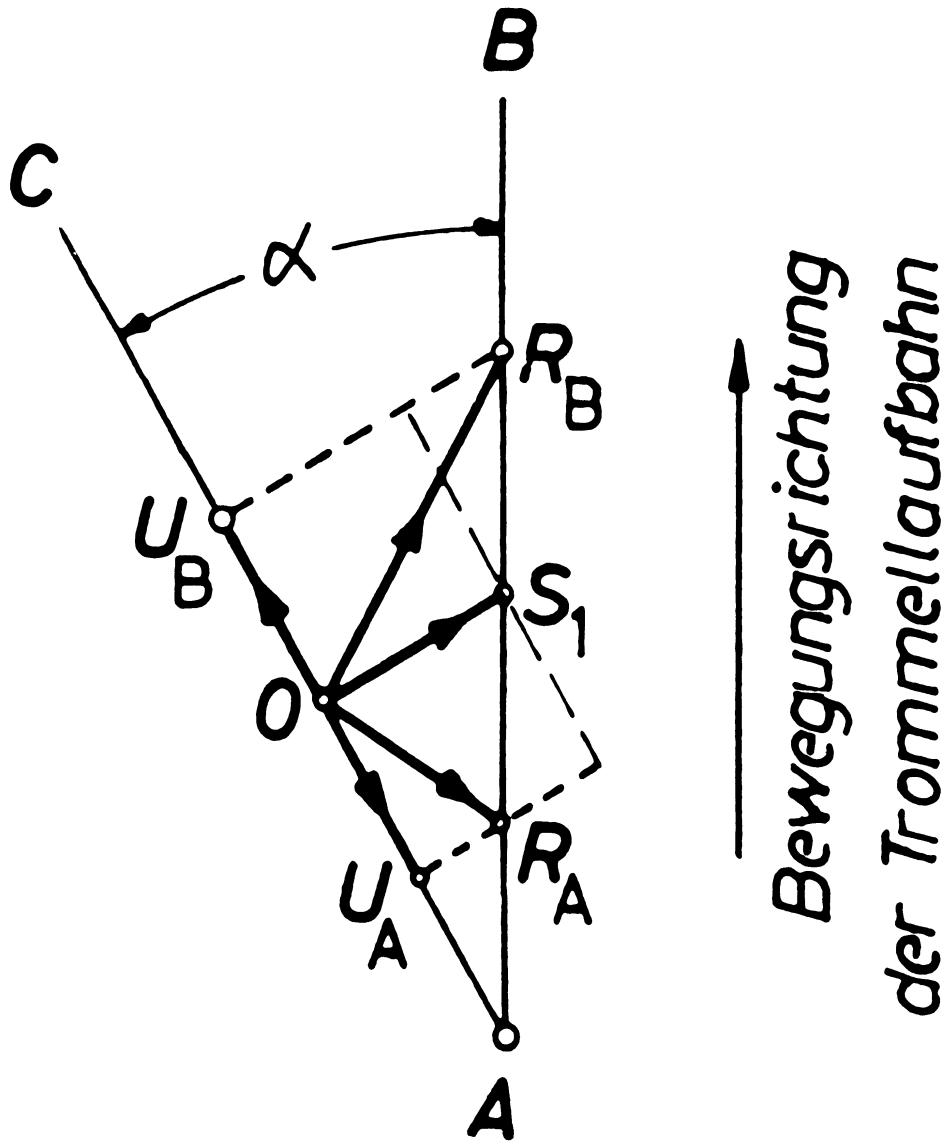

Fig. 29. Simplified representation of what happens in the contact area under steer angle and circumferential force.

2. The maximum transmissible tractive force, the braking force and the maximum side force are in most cases not of the same magnitude.

3. The envelope for the forces transmitted in an arbitrary direction is a circle only for special cases.

4. The deviations from the so-called static friction circle may attain as much as 20%.

5. The circumferential force reaches a distinct static friction value up to steer angles of 5°. After this value it decreases.

We arrive at about the same results if we investigate the influence of the circumferential force on the camber force. The test result for positive and negative camber are given in Fig. 30 for a conventional tire. For both camber directions, we can notice a distinct increase of the camber force under braking forces and a decrease under tractive forces.

Figures 31 and 32 show the behavior of the camber force of two belted tires with asymmetrical side force behavior for $\alpha = 0°$ and U = 0 Kp. The tire in Fig. 31 generates a side force of S = -12 Kp, the one in Fig. 32, a side force of S = + 17 Kp at geometric zero position. In addition, the latter tire was not completely round. Both tires show a completely asymmetric characteristic.

MAXIMUM FRICTION

The idea that the transmissible friction forces on a vehicle tire are independent of the force direction can be true, if the assumption is made that all influences of the parameters like wheel load, air pressure, profile (tread) condition, speed and so on have the same effect on the tire in circumferential direction, as well as in the direction of the side force. However, the measurements performed on the test stand do not agree with this idea:

1. For increasing load the maximum side force increases less than the transmissible circumferential force.

2. The decrease in transmissible circumferential force which has been observed for several types of tires, when the air pressure was increased over 1.5 atu, could not be observed for the maximum side force within the investigated range up to 4 atu.

3. The transmissible circumferential force is different for traction and braking.

4. The speed has a greater influence on the transmissible circumferential force than on the maximum side force.

5. The influence of the tread condition on the side force is mostly greater

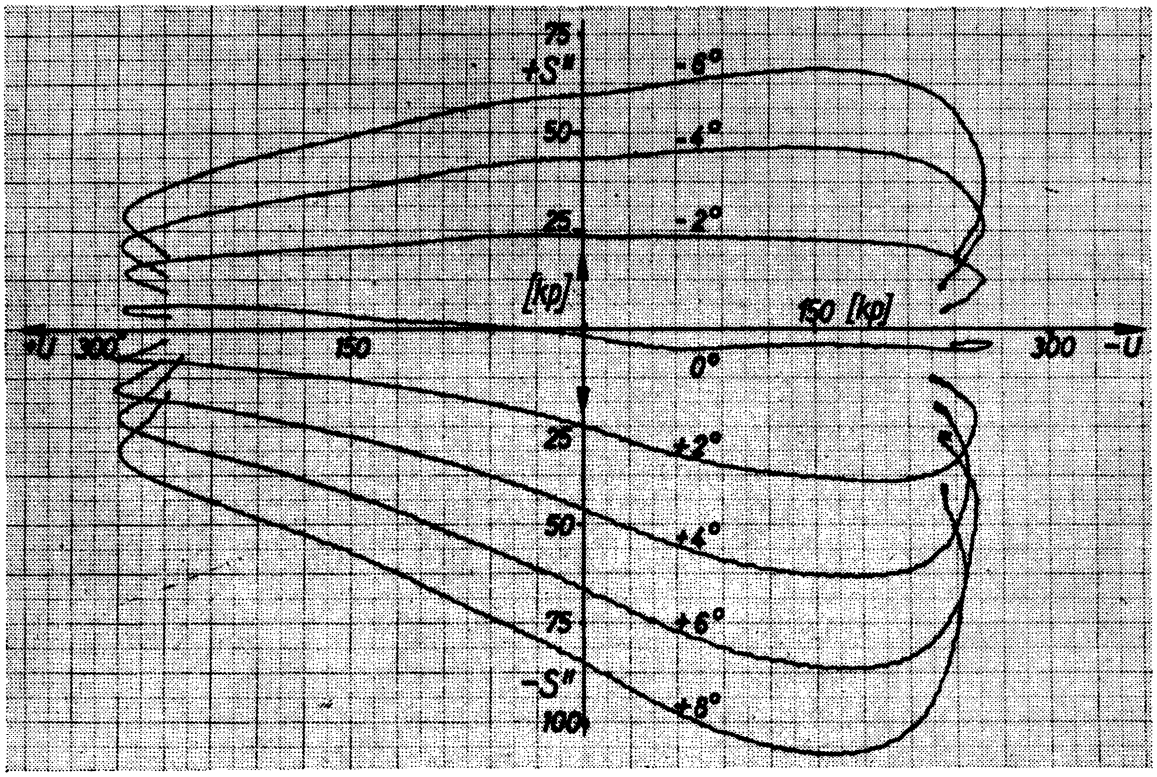

Fig. 30. Camber force S" as a function of tractive and braking force for different camber angles. Conventional tire 6.00-15, profile 60%, rim 4Jx15, G = 300 kg, p = 1.8 atu, V = 50 km/h.

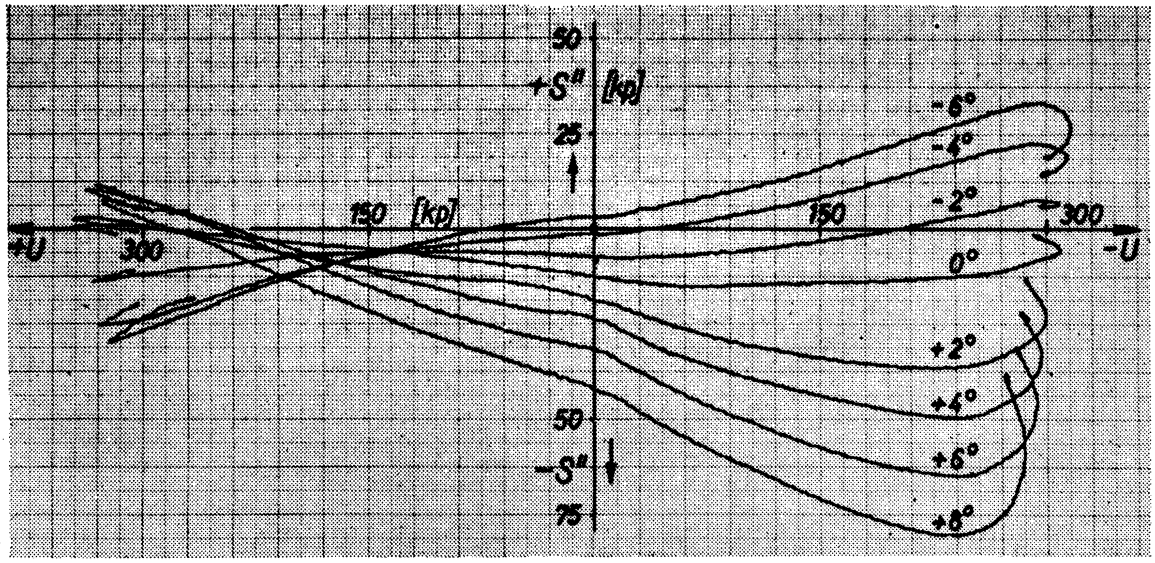

Fig. 31. Camber force S" as a function of tractive and braking force for different camber angles. Belted tire 165R-15, profile 40%. All other data same as in Fig. 30.

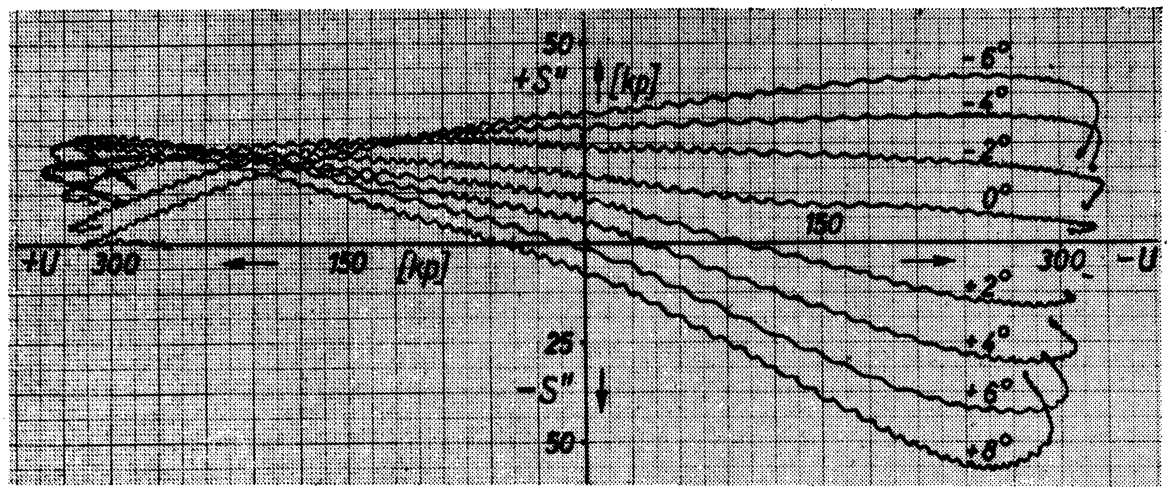

Fig. 32. Camber force S" as a function of tractive and braking force for different camber angles. Belted tire 165R-15, profile 60%. All other data same as in Fig. 30.

than on the circumferential force.

From these observations we must conclude the following:
The transmissible friction forces in their limiting values are with few exceptions, dependent on the direction of the force. The envelopes for the measurements plotted in Fig. 26 to 28 show the dependence of the maximum transmissible friction forces, on the direction of the force for different tire types under a wheel load of 300 Kp and a speed of 50 k /h. By performing several measurements, the influence of the load on the shape of the curve for the transmitted friction forces has been investigated. They are plotted in Fig. 33 to 35 for three different tire constructions. With increasing load, these envelopes become more and more elliptic. If we know the transmissible circumferential force for $\alpha = 0°$ and the maximum side force for U = OKg, we can compute the curve by the formula:

$$S'^2 = \frac{S'_{max}}{U_{max}} \cdot \sqrt{U_{max}^2 - U^2}$$

where U_{max} is the transmissible braking force or the transmissible tractive force at $\alpha = 0°$.

The influence of the speed on the maximum side force, and on the transmissible circumferential force is different. No influence of the speed could be observed for steer angles up to 5 to 6°. Also for larger steer angles the influence of speed is still small. A distinct decrease in side force with increasing speed, could be observed only near the maximum of the side force (Fig. 36). But also, here the influence of speed is smaller than on the transmissible circumferential force.

The decrease is practically linear for the side force as well as for the circumferential force. The curves of equal tread condition, (80%) for the maximum side force, and the transmissible tractive force intersect at a speed of 123 Km/h. At this speed the friction coefficient for this tire under a load of 200 Kp, and an air pressure of 1.8 atu is equal in the direction of the side force (μS_{max}) and in the circumferential direction (μ_{max}).

In particular, for this speed the concept of a friction circle is appropriate. Below this speed we have elliptic curves, (Fig. 37) with their larger semi-axis in circumferential direction. At higher speeds the larger semi-axis lies in the direction of the side force.

These measurements were performed on a tire under traction. For a tire under braking force, or for different tire types, loads, air pressures, tread conditions,etc., the diagram changes as well as the speed for which the friction values μS_{max} and μ_{max} are equal.

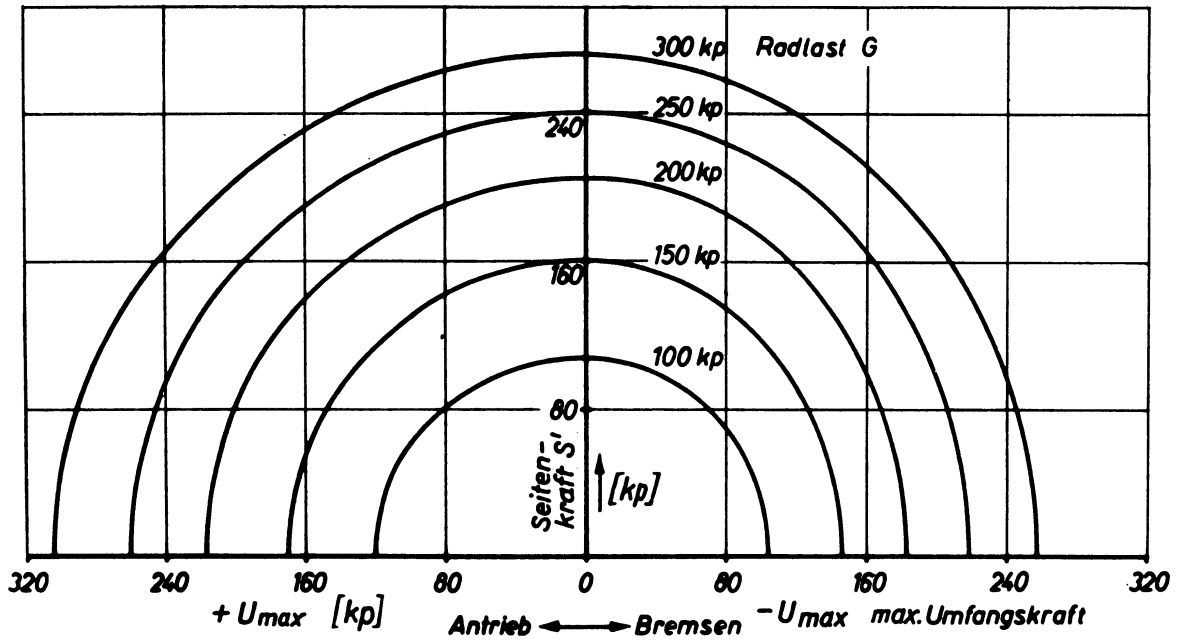

Fig. 33. Friction curves as a function of wheel load, conventional tire 6.00-15, profile 70%, rim 4Jx15, p = 1.8 atu, V = 50 km/h, surface K 80.

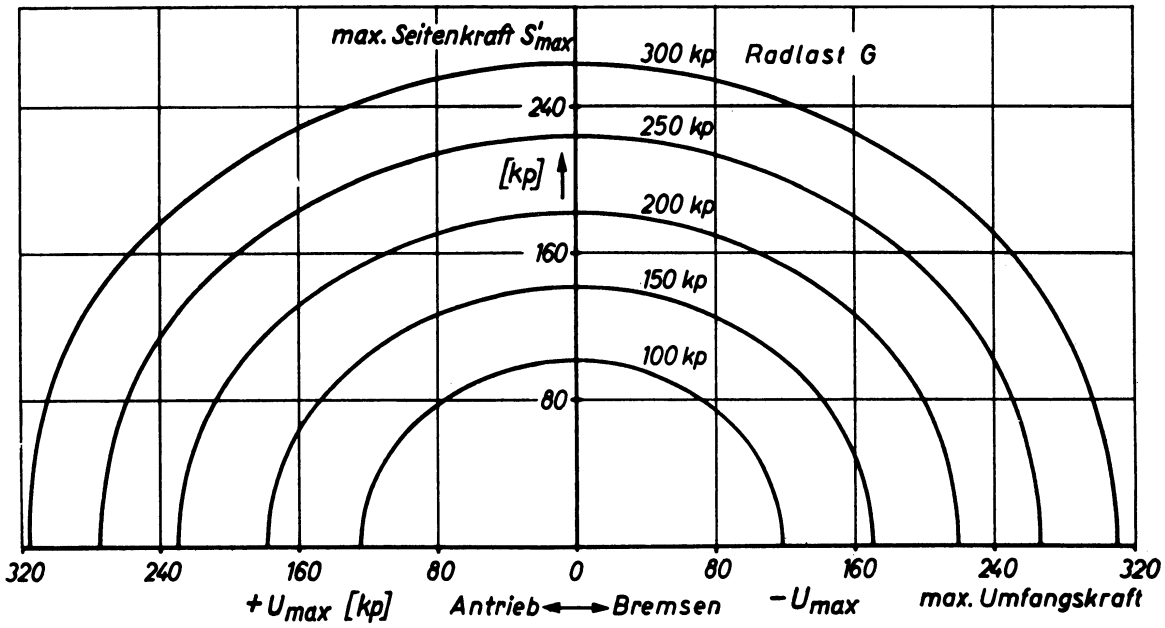

Fig. 34. Friction curves as a function of wheel load, belted tire 165R-15, profile 90%. All other data same as in Fig. 33.

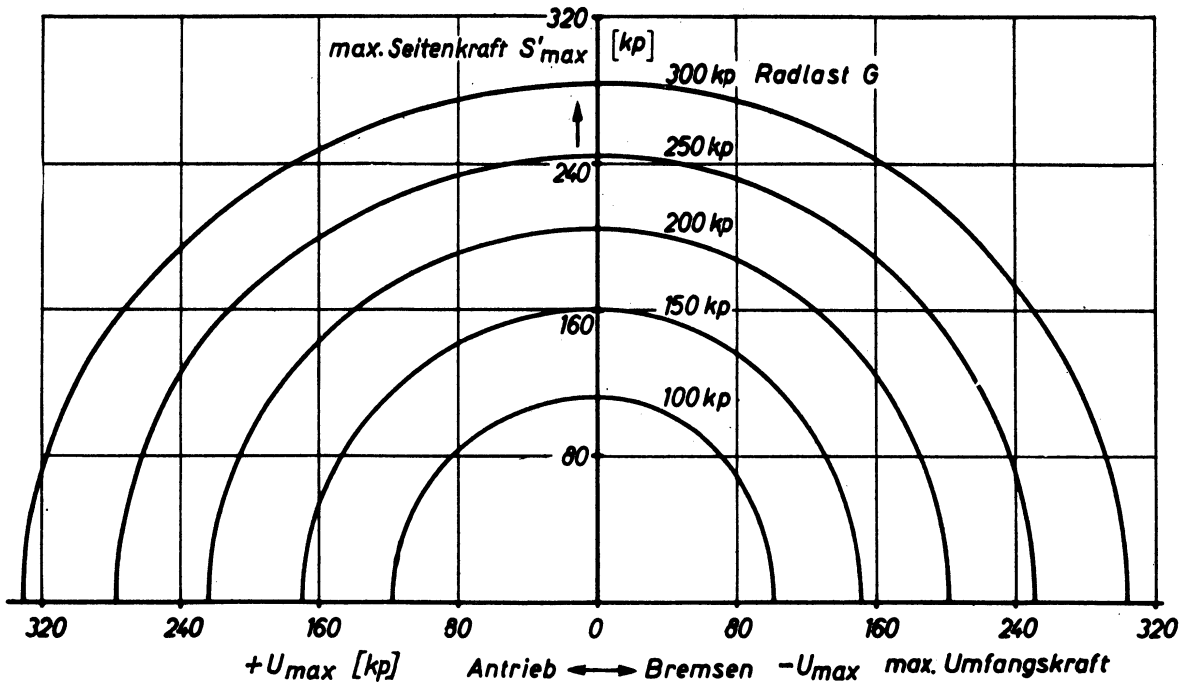

Fig. 35. Friction curves as a function of wheel load, belted tire 165R-15, profile 60%. All other data same as in Fig. 33.

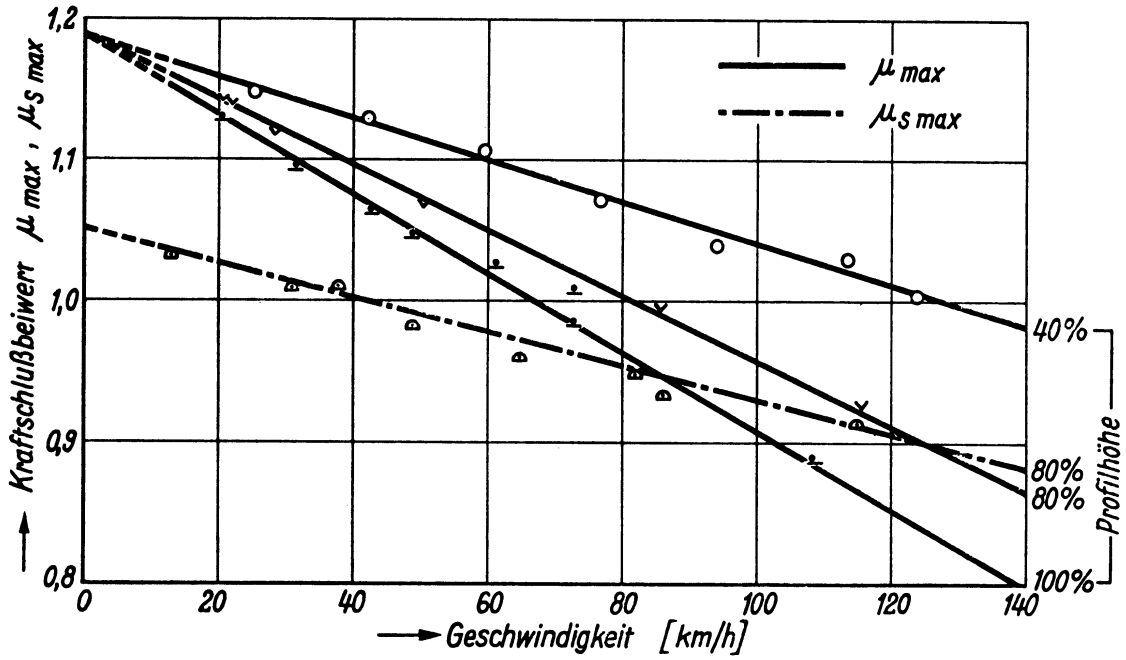

Fig. 36. Influence of the speed on the friction coefficients of transmissible tractive force and maximum size force for different profile (tread) conditions. Belted tire 165R-15, rim 4Jx15, G = 200 kg, p = 1.8 atu, surface K 80.

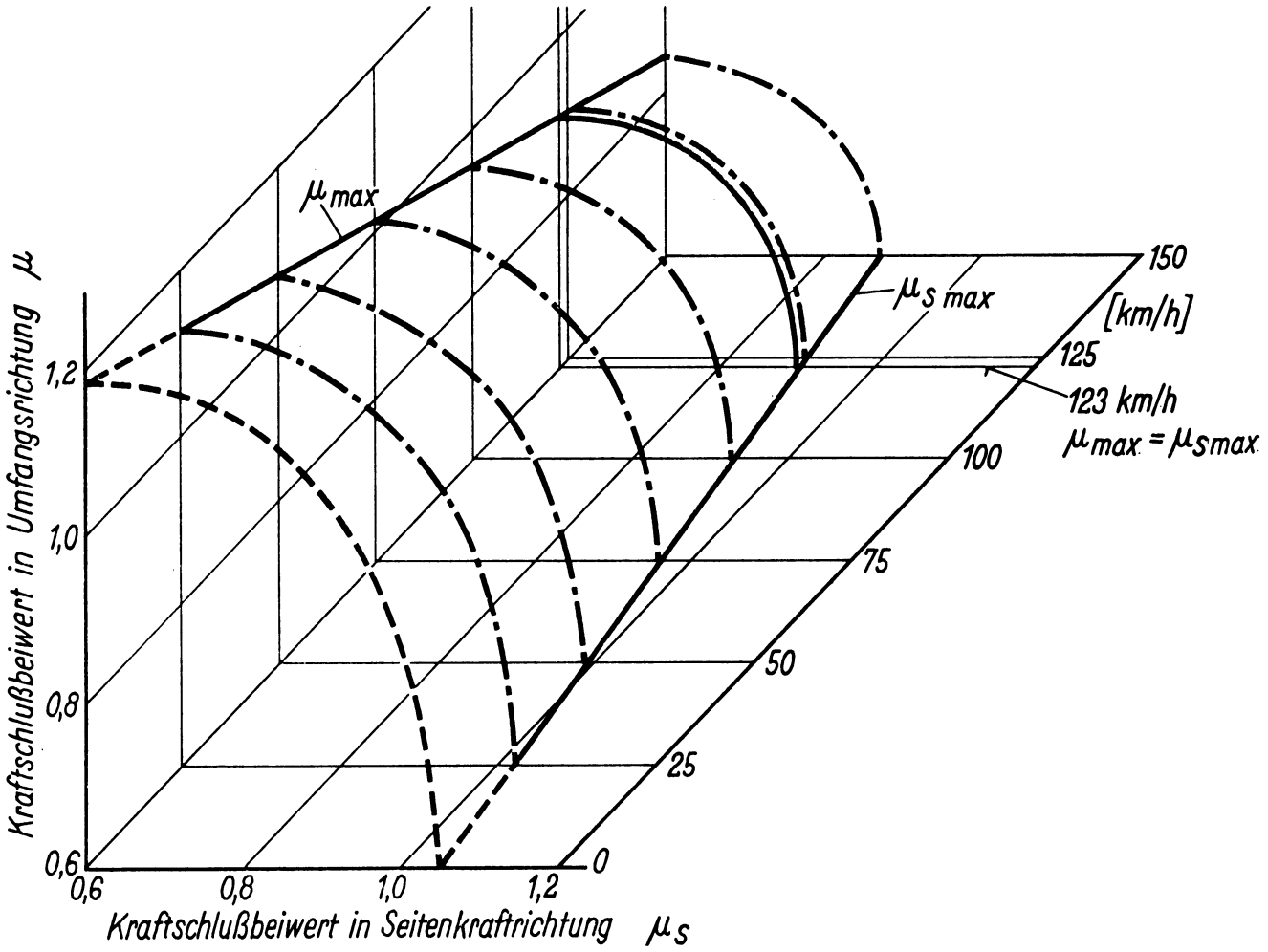

Fig. 37. Friction curves as a function of speed, belted tire 165R-15, profile 80%. All other data same as in Fig. 36. For a speed of 123 km/h we have a friction circle, otherwise the curves are ellipses.

REFERENCES

[1] Bergman, W.: Theoretical Prediction of the Effect of Traction on Cornering Force. SAE Transactions 1961. Auszug in ATZ 64 (1962): Seitenkraft am Luftreifen während des Antriebes

[2] Bode, G.: Kräfte und Bewegungen in der Bodenberührungsfläche rollender Reifen von Lastkraftwagen. Deutsche Kraftfahrtforschung und Straßenverkehrstechnik, Heft 146 (1961)

[3] Brunner, W.: Erwärmung der Reifen von Personenkraftwagen bei hohen Fahrgeschwindigkeiten. Deutsche Kraftfahrtforschung, Heft 2

[4] Bull, A. W.: Der Reifeneinfluß auf das Lenkverhalten. SAE-Journal Vol. 45 (1939) Nr. 2 (übersetzt VW-Literaturdienst)

[5] Buschmann, H., Koeßler, P.: Taschenbuch für den Kraftfahrzeugingenieur, 7. Auflage. Deutsche Verlagsanstalt, Stuttgart 1963

[6] Bussien: Automobiltechnisches Handbuch. Technischer Verlag Herbert Cram, Berlin 1965

[7] Cooper, D. H.: Die Verteilung der Seitenführungskraft und des Schlupfes in der Bodenberührungsfläche von Reifen. Kautschuk und Gummi. 1958, Heft 10, WT 273

[8] Cooper, D. H., Gough, V. E., Hardman, J. H.: Seitenkraft und Seitenverschiebung in der Berührungsfläche zwischen Reifen und Straße. ATZ 63 (1961)

[9] Deininger, W.: Einfluß der Antriebskraft auf die Fahrstabilität von Kraftfahrzeugen. Diss. Technische Hochschule Stuttgart 1963 und ATZ 1965, S. 205 (Auszug)

[10] Dietz, O., Harling, R., Huber, L.: Die Fahrlage des Kraftwagens in der Kurve. Die Fahrtrichtungsstabilität des schnellfahrenden Kraftwagens. Deutsche Kraftfahrtforschung, Heft 44

[11] Drozdow: Entstehung stehender Wellen an Luftreifen bei hohen Rollgeschwindigkeiten. Soviet Rubber Techn. 19 (1960) Heft 12

[12] Förster, B.: Versuche zur Feststellung des Haftvermögens von Personenwagen-Bereifungen. Deutsche Kraftfahrtforschung, Technischer Bericht, Zwischenbericht 22 (1938)

[13] Freeman, C. A.: Experimental Determination of the Effect of Traction on Cornering Force. SAE Paper Reprint, No. 186 B, June 1960

[14] French, G.: Rolle des Reifens in Konstruktions- und Betriebsverhältnissen des Kraftfahrzeuges. ATZ 4 (1955) S. 91/99

[15] Freudenstein, G.: Luftreifen bei Schräg- und Kurvenlauf-Experiment und theoretische Untersuchungen an Lkw-Reifen. Deutsche Kraftfahrtforschung, Heft 152

[16] Gauß, F.: Der Kraftschluß des Reifens und seine Messung. ATZ 10 (1955) S. 294

[17] Gauß, F., Wolff, H.: Über die Seitenführungskraft von Pkw-Reifen. Deutsche Kraftfahrtforschung und Straßenverkehrstechnik, H. 133 (1959)

[18] Gough, V. E.: Reibung von Gummi. Kautschuk und Gummi 1958, Heft 11, WT 303. Straßenbau und Straßenverkehrstechnik, Heft 19, 1962

[19] —: Das Verhalten von Reifen in Kurven. Eine bessere Bestimmungsmethode. Rev. Gen. Du Caoutsch. 32 (1955), Automobile Engineer 44 (1954)

[20] —: Die Seitenführungseigenschaften des Reifens im Kennfeld. Automobile Engineer, April 1954, S. 137/38

[21] Gengenbach, W.: Prüfstand für Fahrzeugreifen. Automobil-Industrie 2 — 1964, S. 101

[22] Hey, F.: Untersuchungen der Längskraftverteilung im Latsch. Deutsche Kraftfahrtforschung, Heft 166, 1963

[23] Hofferberth, W.: Wechselwirkung zwischen Luftreifen und Straße. Straßenbau und Verkehrstechnik, Heft 19, 1962

[24] Huber-Kamm: Einrad-Modellversuche, Führungskräfte zwischen Rad und Fahrbahn bei Antrieb und Bremsung. Forschungsbericht vom Institut für Kraftfahrwesen, Stuttgart 1934

[25] Jante, A.: Fahrtmechanik. Bussien, Automobiltechnisches Handbuch, 2. Band 1965, Kap. 3. 1

[26] Joy-Hartley: Tyre characteristics as Applicable to Vehicle Stability Problems. Inst. Mech. Eng. Proc. Autom. Div. (1953/54) Nr. 6 Auszug in Masch.-Bau und Wärmewirtsch. 11 (1956) Nr. 1 S. 22

[27] Kamm, W., Dietz, O.: Die Seitenführungskraft des gummibereiften Rades bei Antrieb und Bremsung. Deutsche Kraftfahrtforschung, Technischer Bericht, Zwischenbericht Nr. 100/1941

[28] Kamm, W., Schmidt, C.: Das Versuchs- und Meßwesen auf dem Gebiet des Kraftfahrzeugs. Verlag Julius Springer, Berlin 1938

[29] Klaue, H.: Bremswerkuntersuchungen am Kraftfahrzeug. Deutsche Kraftfahrtforschung, Heft 13 (1938)

[30] Kluge, H., Haas: Rollwiderstand von Luftreifen. Deutsche Kraftfahrtforschung, Heft 26/1939

[31] Koeßler, P., Klaue, H.: Der Kraftschluß zwischen Rad und Fahrbahn. ATZ 40 (1937)

[32] Koeßler, P., Menger: Untersuchungen des dynamischen Verhaltens am Kraftfahrzeugreifen. Deutsche Kraftfahrtforschung und Straßenverkehrstechnik, H. 111 (1958)

[33] Kollmann, K.: Nouveau banc d'essai pour l'etude de pneumatiques. Revue Generale du Caoutschouc, Oktober 1959

[34] —: Neuer Prüfstand zur Untersuchung von Kraftfahrzeugreifen. (Auszug aus Revue Generale du Caoutschouc) ATZ 1959, Heft 5

[35] Kremer, H.: Söhne, W.: Die Seitenführungskräfte starrer, nicht angetriebener Räder. Grundlagen der Landtechnik 1957

[36] Kummer, H. W., Meyer, W. E.: Rubber and Tire Friction. Pennsylvania State University. Engineering Research Bulletin B 80 (1960)

[37] Kurz, H.: Seitenführungskraft des Kraftwagenrades bei wechselnder Radlast. ATZ 60 (1958)

[38] Lang, O.: Messung der Seitenführungskräfte am Pkw-Reifen. Dipl. Arbeit am Lehrstuhl für MKL und Kfz-Bau der Technischen Hochschule Karlsruhe 1954

[39] Luetgebrune, H.: Über Messungen der Schräglaufwinkel von Reifen an Kraftwagen bei Kreisfahrt. Kautschuk und Gummi 10 (1957)

[40] Marquard, E.: Über den Rollwiderstand von Luftreifen. ATZ 60 (1958)

[41] Meyer, E. W.: Einige Forschungsergebnisse mit gleitenden Reifen. Vortrag auf dem 10. FISITA-Kongreß in Tokio 1964

[42] Novopolsky, V. I.: Rollwiderstand von Personenwagenreifen bei hohen Geschwindigkeiten. Rev. Gen. du Caoutchouc 36/10 (Okt. 59) und ATZ 62 (1960)

[43] Ogorkiewicz, R. M.: Rolling Resistance. Automobile Engineer 49 (1959)

[44] Riekert, P., Gauß, F.: Untersuchungen über die Führungskräfte von Gummireifen. VDI-Berichte, Bd. 16 (1956) S. 59

[45] Riekert, P., Wolff: Untersuchungen über die Führungskräfte von Gummireifen. ATZ 1 (1956) S. 20

[46] Schmidt, C.: Der Kraftschluß zwischen Reifen und Fahrbahn. ATZ 41 (1938)

[47] Schmihing, H.: Messung der Seitenführungskräfte am Pkw-Reifen unter Berücksichtigung des Sturzes. Dipl. Arbeit am Lehrstuhl für MKL und Kfz-Bau der Technischen Hochschule Karlsruhe 1956

[48] Schuster, R., Weichsler, P.: Der Kraftschluß zwischen Rad und Fahrbahn. ATZ 1935

[49] Thieme, van Eldik: Experimentelle und theoretische Untersuchung der Massenfederungssysteme. FISITA 1960, Elsevier Publishing Company 1960

[50] Tschudakow, E. A.: Der Einfluß der Seitenelastizität der Räder auf die Bewegung des Fahrzeugs. Schriftenreihe des VEB-Verlages, Techn. Band 123, Berlin 1953

[51] Turner: Wellenbildung in Reifen bei hoher Geschwindigkeit. Ref. Hochmol. Ber. 30/5 (1955)

[52] Wehner, B.: Vergleich verschiedener Methoden zur Messung der Straßengriffigkeit. Straße und Autobahn, Heft 6 (1959) S. 201/210

[53] Weil, G.: Über die Reibungswerte zwischen Rad und Fahrbahn. Diss. Technische Hochschule Stuttgart 1934

[54] Wolff, H.: Untersuchungen über die Führungskräfte von Gummireifen. Dt. Kraftfahrtforschung, Techn. Forsch.-Bericht 2 (1956) (Blaues Heft)

[55] Zoeppritz, P., Huber, L., Kamm, W.: Wellenförmige Reifenabnutzung. Deutsche Kraftfahrtforschung, Heft 15

[56] Zoeppritz, P.: Reifen und Fahrbahn in ihrer Wechselwirkung. Bericht über das internat. Kautschuk-Symposium Paris 1959. ATZ Heft 2/1960, S. 20/40